Atmospheric Physics

Adrian Tompkins, ICTP, Trieste, Italy

Email: tompkins@ictp.it

Version release date: June 23, 2016

These course notes and presentations have benefitted enormously from material taken (sometimes even with permission!) from Stephan de Roode, Keith Shine, John Chiang, Vince Larson, Bill Cotton, Ulrike Lohmann, Francesca Di Giuseppe, Denis Hartmann, Stephen Lower, in addition to figures and graphics from many other sources including the IPCC reports and Wikipedia. Apologies to authors of material that have still not been attributed. To my students, please note that brown links are citations, blue are cross-document links and red links are for external web resources. The index and contents page may also be useful. Please contact me for citation corrections, acknowledgments, suggestions and above, corrections to the numerous mistakes!

Contents

Chapter 1

Cloud Physics

1.1 Introduction

Competition between homogeneous and heterogeneous ice mechanisms
LET'S START

Introduction to cloud physics
In all our discussions so far of convection, we have readily assumed that in updraught motions, once saturation is reached cloud drops readily form. However it is not obvious that this is the case. Indeed, we shall see that this is not the case for the formation of ice crystals.

In this part of the course we move to the small scale physics that occurs on the *microscale* of droplets within clouds, known as *cloud microphysics*. What are the processes that we need to consider in clouds therefore?

Cloud processes
We will consider the

- change of phase from water vapour to liquid droplets or ice crystals
- transformation of small cloud droplets to larger rain drops
- freezing of cloud droplets
- formation of ice crystals from water vapour
- advection/falling of the larger sized droplets (precipitation)
- evaporation/sublimation of precipitation and cloud

Cloud particle modes
Condensed droplets of water can obviously have a range of sizes, or droplet radius. However the probability density function describing the droplet sizes is not a smooth function from the very small to the very large (large being a relative term!), but instead we shall see that diverse and discrete cloud processes contrive to produce distinct peaks in the droplets size spectra, termed *modes*. We shall follow the convention of considering each mode as a *bulk quantity*.

For example, Fig. 1.1 shows typical drop size spectra for a range of cloud types (Quante, 2004). We will consider modes of

- cloud drops
- rain drops
- ice crystals
- snow flakes

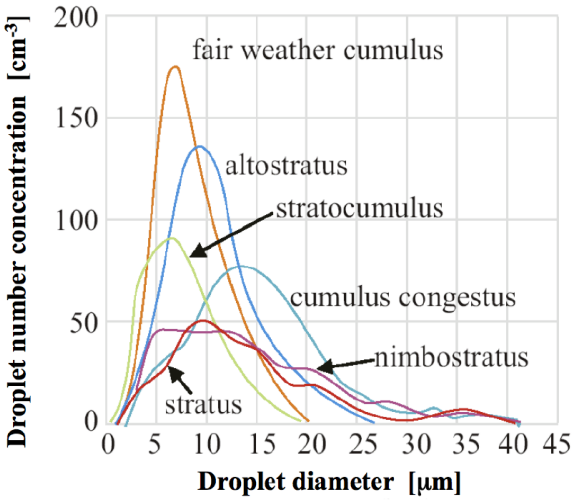

Figure 1.1: Measured drop sizes from various types of clouds, from Quante (2004).

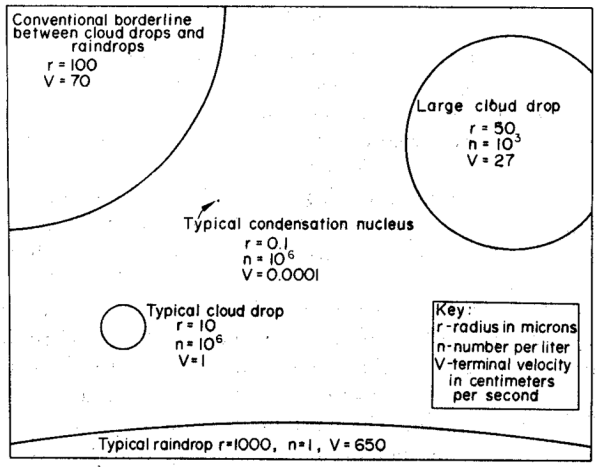

Figure 1.2: Typical drop sizes, from Mcdonald 1958 ?, reproduced from Rogers and Yau (1989).

For ice processes the division is less obvious since ice crystals can form many different shapes or *habits*, with differing radiative and microphysical (e.g. fall-speed) properties despite similar particle sizes which may be treated as a separate category. It is always possible to divide each mode into finer size categories of course, for instance considering small and large cloud ice particles separately. Figure 1.2 shows a schematic of the typical sizes of cloud particles in *warm phase* (i.e. no ice processes involved) clouds. The cloud droplet has a typical radius of 10μm, (a micron=1 μm), 100 times smaller than a typical raindrop. In general we will consider cloud microphysical processes as pathways that can either convert particles from one or more discrete modes to a different particle mode, or can change the mass or size distribution within one particular mode. Figure 1.3 reveals a bewildering array of such processes. A full description of clouds at this level of complexity is beyond the scope of this course, but the diagram reemphasizes the complexity of the task to represent such small-scale complex processes in global climate models with 100km size grid-boxes.

1.2 Cloud drop formation

In our earlier lecture we assumed that supersaturated states could not exist and water vapour in excess of the saturation mixing ratio was immediately condensed into cloud droplets. It is not obvious that this should be the case. We will now consider the effects imports for cloud particle

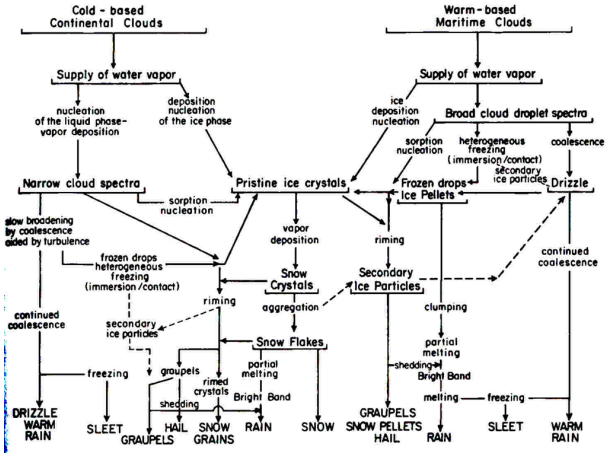

Figure 1.3: Schematic of cloud process pathways between various cloud particle modes (source unknown)

activation.

Water molecules exhibit two types of interactions in the liquid and solid phases: strong covalent bonds within the molecule (O-H bonds) and relatively weak hydrogen bonds between them (Fig. 1.4).

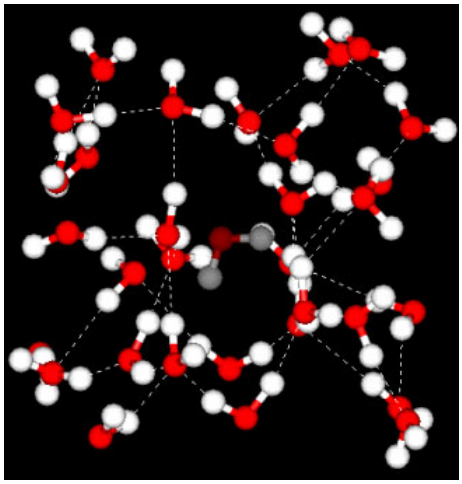

Figure 1.4: Schematic of liquid water structure

Surface tension

A molecule within the bulk of a liquid experiences attractions to neighboring molecules in all directions, but since these average out to zero, there is no net force on the molecule (Fig.1.5). For a molecule that finds itself at the surface, the situation is quite different; it experiences forces only sideways and downward. As a consequence, a molecule at the surface will tend to be drawn into the bulk of the liquid. But since there must always be some surface, the overall effect is to minimize the surface area of a liquid. This is what creates the stretched-membrane effect known as *surface tension*, $\sigma_{l,v}$.

The surface tension is the free energy per unit surface area of the liquid and can be viewed as the work per unit area required to extend the surface of liquid at constant temperature. The formation of a liquid drop needs an energy:

$$\Delta E = 4\pi r^2 \sigma_{l,v} \tag{1.1}$$

r is the drop radius. $\sigma_{l,v} \approx 7.5 \times 10^{-2} Nm^{-1}$ for usual conditions. The distinction between molecules located at the surface and those deep inside is especially prominent in water, owing to the strong hydrogen-bonding forces. Thus, compared to most other liquids, water also has a high surface tension. The geometric shape that has the smallest ratio of surface area to volume is the

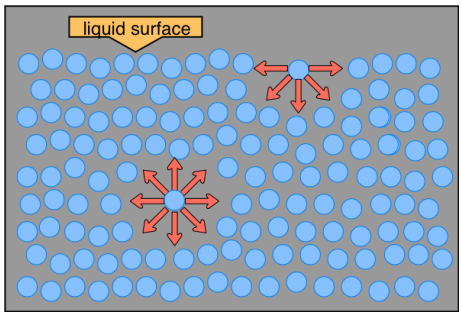

Figure 1.5: Schematic of the surface tension effect (source: www.chem1.com)

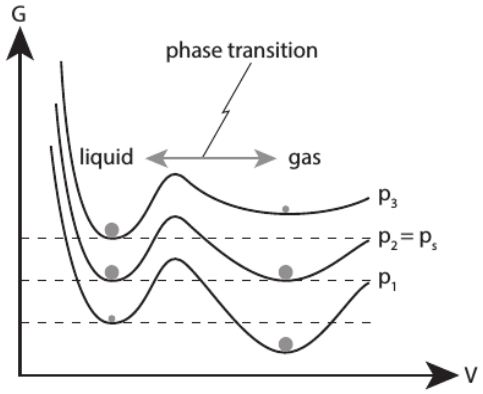

Figure 1.6: Schematic of Gibbs free energy as a function of the substance volume at three different pressures that are respectively less than, equal, or exceed the saturation pressure p_s. Local equilibria (energy minima) are shown with circle, with the larger circles indicating absolute minima. From Kashchiev (2000)

sphere, so very small quantities of liquids tend to form *spherical drops*. The fact that energy is required to form the drop interface implies an energy barrier. The implication is that phase transitions are *not* spontaneous, even if the Gibbs free energy would be lower as a result.This is illustrated in Fig. 1.6. Even if $e > e_s$ and thus liquid is the "preferred" phase, exhibiting a Gibbs energy minimum, phase transition requires an energy barrier to be overcome. There is no thermodynamical reason why a system in a local stable state may increase its Gibbs free energy and cross the barrier to change phase. Thus processes of phase transition require concepts from statistical mechanics that describe molecular-scale fluctuations of the system, in addition to thermodynamics. Random fluctuations may lead to some molecules overcoming the Gibbs energy barrier. The size of the barrier depends on the path. For example, in Fig. 1.6 we can view the path along the line $p = p_s$ as the result of all molecules changing phase from gas to liquid, which would involve a high energy barrier. Instead, the barrier energy is much lower if the new phase occurs as the result of the formation of a small stable nucleus, involving a subset of n molecules (Fig. 1.7). Hence phase transition in this way is referred to as a *nucleation event* . The nucleation event in this example is referred to as *homogeneous*, since no foreign surface is present to lower the energy barrier.

1.2.1 The energy barrier and Kelvin's equation

We now examine the energy barrier associated with the formation of a nucleus of n molecules in the new liquid phase formed from a parent phase of N molecules as illustrated in Fig. 1.7. The Gibbs State 1 has a Gibbs free energy of $G_1 = Ng_v$, where g_v is the Gibbs free energy per molecule in the vapour phase. $G_2 = (N - n)g_v + G(n)$, where $G(n)$ is the Gibbs free energy of the liquid phase nucleus, and has two contributions: $G(n) = ng_l + G_{surf}(n)$. The first term is the Gibbs free energy associated with the molecules in the liquid phase, while $G_{surf}(n)$ represents the work that has to be done to form a surface around a volume containing n molecules. The work needed to

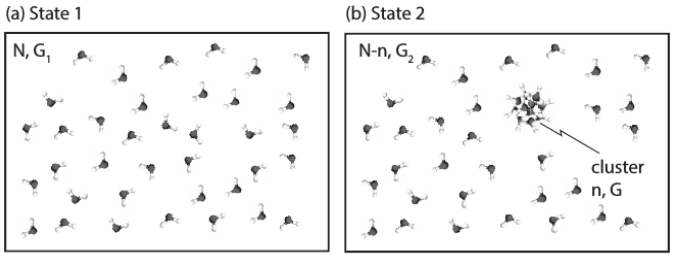

Figure 1.7: Schematic of the a nucleation event (source: Lohmann U, ETH)

form the cluster is therefore

$$G_2 - G_1 = \Delta G = n(g_l - g_v) + G_{surf}(n) \tag{1.2}$$

To calculate the first term, we integrate dg from e_s for liquid to e the vapour pressure of the surroundings at constant temperature:

$$g_v - g_l = \int_{e_s}^{e} dg = \int_{e_s}^{e} v dp = \int_{e_s}^{e} \frac{kT}{p} dp \tag{1.3}$$

where we use $pv = kT$ for a single molecule to derive the final term. Integration of this gives $g_v - g_l = kTln(e/e_s)$ (refer to derivation of Clausius Clapeyron in the thermodynamics notes). This is per molecule, thus for n molecules we can write

$$n(g_l - g_v) = nkTln(S) = \frac{R_v T}{v_l} \frac{4}{3} \pi r^3 ln(S), \tag{1.4}$$

where v_l is the specific volume of liquid water and r is the nucleus radius, and $S = \frac{e}{e_s}$. The second term of eqn. 1.2 should account for the pressure difference within the droplet, but liquid droplets are approximately incompressible, and thus the energy is given by Eqn 1.1

$$G_{surf} = 4\pi r^2 \sigma_{l,v} \tag{1.5}$$

Combining eqns 1.4 and 1.5, we obtain the equation for Gibbs free energy for a cluster formation in a parent phase.

$$\Delta G = \underbrace{4\pi r^2 \sigma_{l,v}}_{\text{surface term}} - \underbrace{\frac{4R_v T}{3v_l} \pi r^3 ln(S)}_{\text{volume term}} \tag{1.6}$$

The first term on the right is referred to as the *surface term* and the second is the *volume term*. Note the different r dependency. We assumed a constant temperature in this derivation and thus latent heating is neglected. Equation 1.6 is illustrated in Fig. 1.8. If $S < 1$ then the volume and surface terms are both positive, and ΔG increases monotonically with r. If $S = 1$ the volume term is zero, but ΔG increases due to the surface term. For $S > 1$, there is a peak value of ΔG occuring at a critical radius, which is an unstable equilbrium and marks the magnitude of the energy barrier. If the drop radius is smaller than the critical radius the drop will tend to dissipate, while for a radius exceeding this critical threshold the drop should grow (in theory infinitely). To calculate the critical radius, we can differentiate eqn. 1.6 to get $\frac{dG}{dr}$ (*exercise!*) and then set $\frac{dG}{dr} = 0$. The critical radius r_c is then

$$r_c = \frac{2\sigma_{l,v} v_l}{R_v T ln(e/e_s)} \tag{1.7}$$

Thus we have seen that there is an energy barrier resulting from the surface tension of a droplet, which was defined as the work per unit area required to extend the surface of a drop. A more physical interpretation for this is as follows. We saw that surface tension resulted from the asymmetry of the forces of attraction at the drop surface. Work is thus required to bring a molecule from the interior of a drop to its surface, as it requires bonds to be broken. A molecule on the surface will then require less energy to overcome the remainding binding H-bonds and be released in the gas phase. The smaller the droplet, the more curved the surface and the stronger this effect becomes.

Saturation over a curved surface

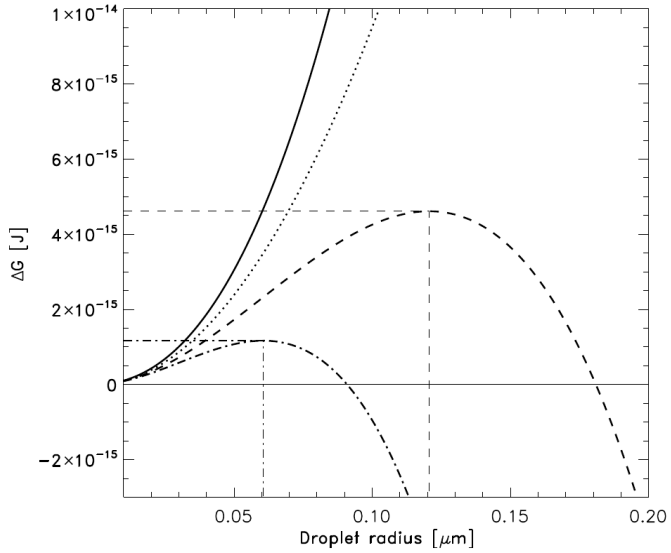

Figure 1.8: Gibbs free energy for homogeneous water droplet formation of radius r at T=273.15K for saturation ratios of S= 0.99 (solid), 1 (dotted), 1.01 (dashed) and 1.02 (dot-dash). The critical radii of 0.06 and 0.12 μm are shown for the latter two saturation values (source U. Lohmann).

The relationship given earlier in the thermodynamics course for the saturation vapour pressure was for a *planar water surface*. We have seen that on the scale of a cloud droplet the curvature of the surface is sufficient to reduce the number of (attracting) neighbouring molecules.

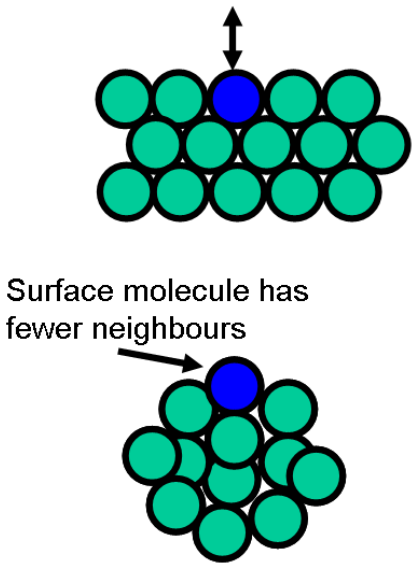

Figure 1.9: Schematic of evaporation process showing how water molecules have fewer neighbours in a curved drop relative to a planar surface.

The saturation vapour pressure is thus higher over a *curved surface*. The saturation vapour pressure of a liquid droplet of radius r given by inverting Eqn. 1.7, thus giving the minimum supersaturation $S = e/e_s$ that is required for a droplet of radius r to exist. :

$$\frac{e_s(r)}{e_s(\infty)} = \exp\left(\frac{2\sigma_{l,v}}{r\rho_l R_v T}\right), \tag{1.8}$$

[1]. This is known as the *Thomson* or *Kelvin* effect. Although T is in the denominator on the RHS, e_s is also a function of T and the temperature dependence is in fact weak. Note that the surface tension in the above equation refers to the surface tension of a pure liquid water droplet in water vapour. Presence of aerosols will change this value. Moreover, the above formulations are also valid for other phase changes, e.g. ice germ formation in a liquid, but the surface tension value are less well defined from experimentation. We can simplify eqn. 1.8 to

$$\frac{e_s(r)}{e_s(\infty)} = \exp\left(\frac{a}{rT}\right), \tag{1.9}$$

where $a = 2\sigma_{l,v}/R_v\rho_L$ which is (almost) constant at 3.3×10^{-7} m K.

The right hand side of the expression can be usefully approximated to

$$\frac{e_s(r)}{e_s(\infty)} \approx 1 + \frac{a}{rT}, \tag{1.10}$$

Homogeneous nucleation of liquid droplets

A chance collision of molecules to form a droplet is called *homogeneous nucleation.*

Let us consider such an event involving a relatively rare event: the chance collision contemporaneously of N =183 molecules of water vapour.

To calculate the radius of this newly formed droplet we note that the droplet volume is given by

$$V = \frac{4}{3}\pi r^3 = \frac{m_v N}{N_a \rho_L}. \tag{1.11}$$

Recall that the molecular weight m_v is the mass per mole, while N_a is the number of molecules per mole, thus $\frac{m_v}{N_a}$ is the mass per molecule.

Solving eqn. 1.11 for r (*exercise*), tells us that the droplet of N=183 molecules has a radius of approximately 10^{-3} μm. At a temperature of 273K, the ratio of the equilibrium vapour pressure $e_s(r)$ is three times greater than the value over a planer surface $e_s(\infty)$. The rate of growth of the droplet is proportional to the difference $e - e_s(r)$. If $e < e_s(r)$ then the droplet will evaporate, while it will grow if $e > e_s(r)$. If we define the saturation ratio S as

$$S = \frac{e}{e_s(\infty)} \tag{1.12}$$

so that S =3 equates to a relative humidity of 300%, then for the nascent droplet to grow would require a saturation ratio of S >3. *Q: Do we observe such values of relative humidity?*. In fact, such high values are never measured in the atmosphere, thus homogeneous nucleation is not a relevant mechanism for cloud formation. So what is it?

Aerosols

Aerosols in the atmosphere can range in size from 10^{-4} to 10 μm radius with particle concentrations also widely varying from 10^3 cm^{-3} in a remote location to $> 10^5$ cm^{-3} in an urban environment such as London.

There are a number of *natural and anthropogenic* sources for aerosols:

- mineral soil dust
- sea salt (e.g. Fig. **??**)
- gas to particle conversion SO_2 →sulphate aerosols
- combustion of fossil fuels / biomass burning

Small aerosols with radii < 0.2 μm are referred to as *Aitken particles*, 0.2 < r < 2 μm are *large aerosols*, and r > 2 μm are *giant aerosols*. Both *dry deposition* (sedimentation) and *wet deposition* (removal by precipitation) are the sinks of aerosols, with a typical aerosol lifetime being around 1 week.

[1] We will use notation $e_s(r) = e_s^r$ interchangeably.

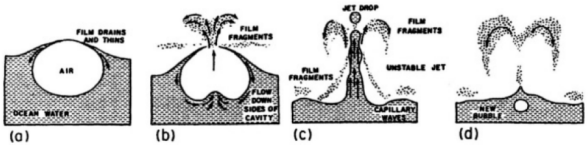

Figure 1.10: Formation of sea salt aerosol, from Pruppacher and Klett (1997).

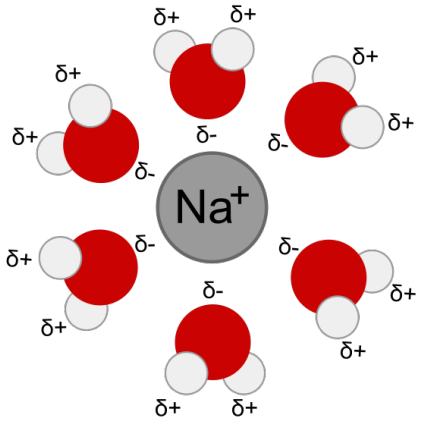

Figure 1.11: Schematic showing dissolution of sodium ion in water (wikipedia)

Heterogeneous nucleation of liquid droplets

Many aerosols in the atmosphere are hydrophilic (A hydrophilic molecule is one that has a tendency to interact with or be dissolved by water) and thus water molecules can collect on their surface. Clouds can thus form by a process known as *heterogeneous nucleation*, where water molecules collect on a foreign substance. These hydrophilic aerosols are called *Cloud Condensation Nuclei* or CCN. These CCN are always present in sufficient numbers in the lower and middle troposphere to initiate cloud growth.

CCN aerosols can be insoluble but *wettable*, which means that the surface tension between their nucleating surface and water is sufficiently low and water can form a spherical cap completely surrounding the aerosol. Thus the physics of drop nucleation is the same as for pure water. Only large or giant aerosols ($r > 0.2$ μm) generally have a low enough curvature to form cloud droplets at observed supersaturations. However, aerosols can instead be *soluble*, in which case aerosols with much smaller radii can act as CCN. *Solvation*, also sometimes called *dissolution*, is the process of attraction and association of molecules of a solvent with molecules or ions of a solute.As ions dissolve in a solvent they spread out and become surrounded by solvent molecules (Fig. 1.11).

The solution term

The presence of dissolved substances implies that the some water molecules are replaced from the droplet surface (Fig. 1.12). Thus the saturation vapour pressure is reduced for a *solute*.

If $e_s(sol)$ is the saturation vapour pressure over a solute and n_w and n_s are the number of water and solute molecules, respectively, then the fraction of surface which is occupied by water molecules is simply:

$$\frac{e_s(sol)}{e_s^\infty} = \frac{n_w}{n_w + n_s} = \left(1 + \frac{n_s}{n_w}\right)^{-1} \simeq 1 - \frac{n_s}{n_w}, \tag{1.13}$$

where the final approximation assumes $n_s \ll n_w$. In a droplet the number of water molecules is proportional to r^3, thus for a fixed mass of aerosol this effect adjust the saturation vapour pressure by a factor

$$\frac{e_s(sol)}{e_s^\infty} = 1 - \frac{b}{r^3} \tag{1.14}$$

where b is a constant that depends on the aerosol mass and type. The curvature (1.10) and solute (1.14) effects can be combined to give the resultant equilibrium curve referred to as the *Köhler curve* given by:

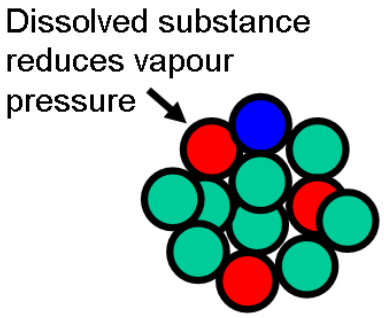

Figure 1.12: Schematic showing how saturation vapour is instead reduced when there are molecules of dissolved substance (red) present in the droplet.

$$\frac{e_s^r(sol)}{e_s^\infty} = \left(1 - \frac{b}{r^3}\right) \exp\left(\frac{a}{rT}\right) \approx \left(1 + \underbrace{\frac{a}{rT}}_{\text{curvature term}} - \underbrace{\frac{b}{r^3}}_{\text{solute term}}\right) \tag{1.15}$$

Figure 1.13 shows a normalized curve, and the actual shape depends on the mass and type of solute. For a solute formed with 10^{-16} g of ammonium sulphate the solution term is ineffective for radii above 0.3 μm. Due to the r^3 factor the solute term dominates at small droplet radii.

If RH increases starting from a low value, water vapour start to condense on aerosol parcels as

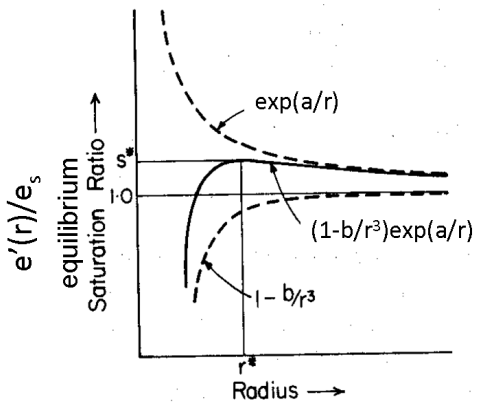

Figure 1.13: Köhler curve for the equilibrium saturation vapour pressure for a liquid solute droplet.

RH reaches about 80% (S =0.8), referred to as *haze* particles. At these small radii the droplet is stable as an increase in RH will cause the haze particle to grow until a new equilibrium radius is reached. However, if the RH continues to increase a critical radius R^* is reached at the critical supersaturation S^* value at which the droplet becomes unstable, and grows rapidly by diffusion. The droplet is said to be *activated*. It is the haze particles that are responsible for reducing visibility on a sunny (humid) day.

In summary, about 10 to 20% of aerosols over oceans can act as CCN, while over land only about 1% can act as CCN. Nevertheless, the total concentration of CCN is still higher over land with a typical value of 500 cm^{-3} compared to 100 cm^{-3} over oceans, but these numbers are highly temporarily and spatially variable. Therefore a cloud air parcel brought to saturation over ocean shares the available water between fewer CCN, so we would expect fewer but larger cloud droplets. The consequence of this is that maritime clouds are more likely to rain. We will see that with larger droplets it is easier to grow raindrops.

1.3 Diffusional growth

Diffusional Growth of droplet

Once a cloud particle is activated it grows rapidly by diffusion of water vapour. As is usual, the local diffusive flux is assumed proportional to the vapour gradient. Integrated over a sphere of radius n (Fig 1.14) the total diffusive flux F (kg s^{-1}) is:

$$F = 4\pi n^2 D \frac{d\rho_v}{dn}, \tag{1.16}$$

where D is the diffusion coefficient ($\approx 2.2 \times 10^{-5}\mathrm{m}^2 s^{-1}$ at 273K) and ρ_v is the vapour density.

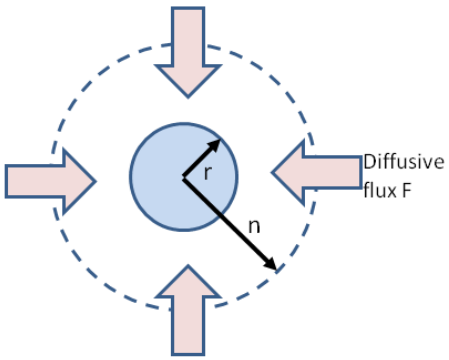

Figure 1.14: Sketch of diffusion growth of a cloud drop.

In a steady state the diffusion rate is balanced by rate of increase of mass of droplet M:

$$\frac{dM}{dt} = 4\pi n^2 D \frac{d\rho_v}{dn}. \tag{1.17}$$

We will assume that the growth is constant. Thus

$$\frac{dM}{dt} \int_r^\infty \frac{dn}{n^2} = 4\pi D \int_{\rho_v(r)}^{\rho_v(\infty)} d\rho_v. \tag{1.18}$$

giving

$$\frac{dM}{dt} = 4\pi D r(\rho_v(\infty) - \rho_v(r)) \tag{1.19}$$

We want the rate of change of radius, so we need the expression

$$M = \frac{4}{3}\pi r^3 \rho_L, \tag{1.20}$$

which we differentiate to give

$$\frac{dM}{dt} = 4\pi r^2 \rho_L \frac{dr}{dt}. \tag{1.21}$$

Substituting (1.21) into (1.19) gives

$$\frac{dr}{dt} = \frac{D}{\rho_L r}(\rho_v(\infty) - \rho_v(r)). \tag{1.22}$$

We now use the ideal gas law ($e = \rho_v(\infty) R_v T$) to change the density to vapour pressure, noting that at the droplet surface the air is exactly saturated:

$$\frac{dr}{dt} = \frac{D}{\rho_L r R_v T}(S e_s^\infty - e_s^r(sol)) \tag{1.23}$$

Now we use our earlier approximate expression for the Köhler curve given in (1.15):

$$\frac{dr}{dt} = \frac{D e_s^\infty}{\rho_L r R_v T}(S - 1 - \frac{a}{rT} + \frac{b}{r^3}) \tag{1.24}$$

This equation is not tractable, but we can solve for $r > 1\mu$m, with the subsequent simplification:

$$\frac{dr}{dt} \simeq \frac{De_s^\infty}{\rho_L r R_v T}(S-1) \tag{1.25}$$

This expression is approximate and ignores an important effect. We have neglected the fact that *latent heat is warming the droplet*, and to be strict the expression should account for the diffusion of heat *away* from the droplet. This "complication" reduces the droplet growth rate very roughly by a factor of 2.

Availability of water vapour
For a hypothetical cloud parcel there are two main terms that affect the supersaturation (or equivalently relative humidity):

- increase due to the parcel cooling: rate proportional to the parcel velocity
- decrease due to the diffusion process

The evolution of an air parcel containing a spectra of diverse CCN can be calculated numerically using a Lagrangian *parcel model* (see Ren and Mackenzie, 2005, for an example in ice clouds). We will consider the hypothetical evolution of the parcel:

1. All CCN start to form haze particles at $RH \approx 80\%$,
2. the larger droplets formed on giant CCN (and thus have lower activation S) become activated first.
3. These giant nuclei are few, thus have limited effect on the water availability, RH continues to increase,
4. and we start to activate drops with higher activation S^*. There are many of these and thus water vapour is consumed, eventually balance is reached where S is at a maximum.
5. After this point particles with lower S^* will continue to grow, while those with higher S^* will decay as S decreases.

The final points to note are that

- The maximum supersaturation between (0.1 to 0.5%) occurs within 10 to 100 metres of cloud base,
- S_{max} defines the number concentration of cloud droplets, and is thus also determined close to cloud base,
- higher updraught speeds give higher S_{max}, thus higher number of activated droplets leading to a higher number of final cloud droplets,
- Growth of cloud droplets from an initial aerosol of 0.5 μm takes only a few seconds explaining why the cloud base is *well defined*,
- Calculated drop size spectra from modelling this process are *narrower* than observed (i.e. less size variability). This is because we have neglected the processes of cloud mixing and coalescence of droplets.

Time taken for diffusional growth
We have an expression for the rate of change of r as a function of time and supersaturation. If we assume S is time-independent we can find out how long it takes to grow cloud droplets of a certain size by the diffusion process by integrating (1.25).

This gives (*exercise: check!*)

$$t = \frac{\rho_L R_v T}{2De_s^\infty(S-1)}(r^2(t) - r^2(0)). \tag{1.26}$$

If we take an example of T=284K and $r(0)$=0.5 μm and $S-1$ =0.002 (a *supersaturation* of 0.2%) then table 1.1 gives the time taken to grow a cloud droplet of the given sizes *Which size is a cloud*

r (μm)	1	5	10	100
t (seconds)	1	36	150	15000

Table 1.1: Time taken to grow a cloud drop of given radius by diffusion.

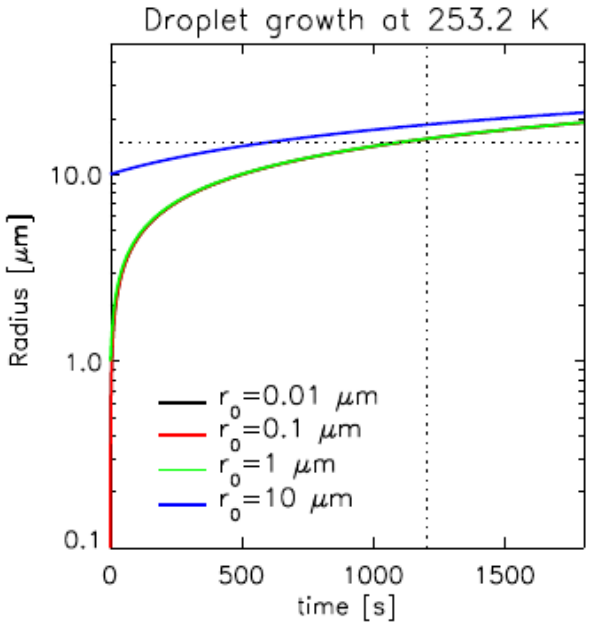

Figure 1.15: Diffusion growth curves, from Lohmann U..

droplet? Can drops grow by diffusion? The nonlinearity of the diffusional growth is emphasized in Fig. 1.15. We recall that 10 μm was a typical cloud radius and thus growth by diffusion *is* fast enough to produce such droplets. However 100 μm is a small raindrop size, and it is seen that over 4 hours are required to achieve this initial raindrop, far longer than the observed life-cycles of precipitating clouds.

1.4 Terminal velocity of particles

Terminal velocity

We now introduce the concept of the terminal fallspeed of particles in a simplified way. The terminal velocity is achieved when the force due to gravity $F = \frac{4}{3}\pi r^3 g(\rho_L - \rho)$ is balanced by the drag on the droplet.

The drag strongly depends on the drop size, as seen in Fig. 1.16. The drag on a droplet is related to the particle velocity V and the radius r and can be divided into three regimes, leading to three distinct terminal fall speed V_t relationships:

- $r < 30\mu$m: Drag $\propto Vr$ giving $V_t = X_1 r^2$ where $X_1 \sim 1.2 \times 10^8 \text{s}^{-1}$ m^{-1}.
- $30 < r < 1000\mu$m: Drag $\propto Vr^2$ giving $V_t = X_2 r$ where $X_2 \sim 8 \times 10^3 \text{s}^{-1}$.
- $r > 1000\mu$m: Drag $\propto V^2 r^2$ giving $V_t = X_3\sqrt{r}$ where $X_3 \sim 250 \text{s}^{-1}$ m$^{0.5}$.

Table 1.2 gives typical fallspeeds as a function of radius. From these fallspeeds we notice two

r (μm)	1	10	20	100	1000
V_t (m s^{-1})	1.2×10^{-4}	0.012	0.048	0.8	8

Table 1.2: Time taken to grow a cloud drop of given radius by diffusion.

facts:

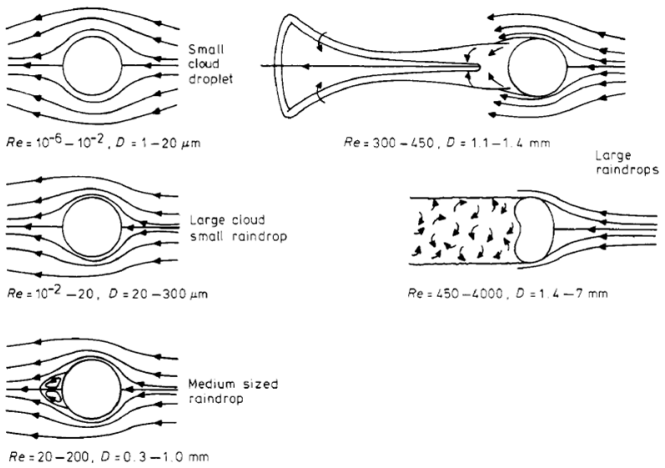

Figure 1.16: Changes in the air flow patterns round falling water drops as the Reynolds number increases (source: Mason, 1978)

- The fallspeed of typical cloud droplets (2 to 20 μm) is negligibly small compared to typical updraught and downdraught velocities, with a 10 micron droplet requiring a day to fall 1km. This means that to a good approximation we can assume that cloud droplets are in suspension in the air.

- The differential terminal fallspeeds also implies that larger droplets falling faster than smaller ones may collide and collect smaller droplets during their descent (see schematic in Figs. 1.17)

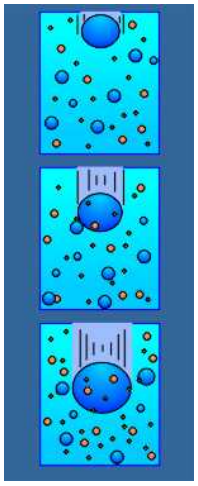

Figure 1.17: Schematic of larger raindrops colliding with smaller drops during descent (source hrefwww.islandnet.comislandnet.com).

The sequence of laboratory photos shown in Fig. 1.18 show a droplet collision and cohesion event.

1.5 Collision and coalescence

We consider a large drop of radius R is falling through a cloud of smaller droplets radius r. If we take a simple view and assume that any small droplet in the path of the large droplet comes into contact and is *collected* (as in the sequence of Fig. 1.19, the volume of droplets collected per unit time is $\pi(R+r)^2(V-v)$. The liquid water content of the small droplets is $L = q_l\rho$ in kg m^{-3},

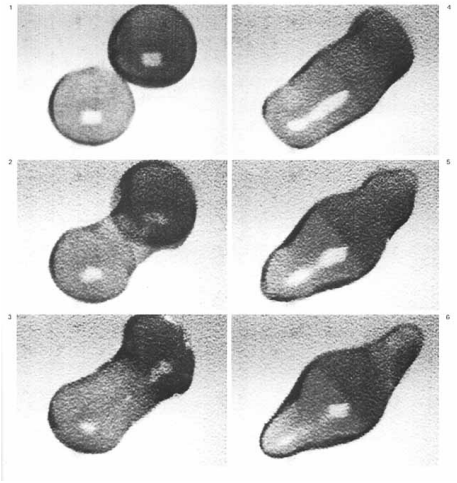

Figure 1.18: Sequence of shots showing droplet collision and subsequent cohesion (source unknown)

giving a mass accumulation rate of

$$\frac{dM}{dt} = L\pi(R+r)^2(V-v) \tag{1.27}$$

We will simplify the equation by assuming $R >> r$ and $V >> v$, and then use (1.21) which we

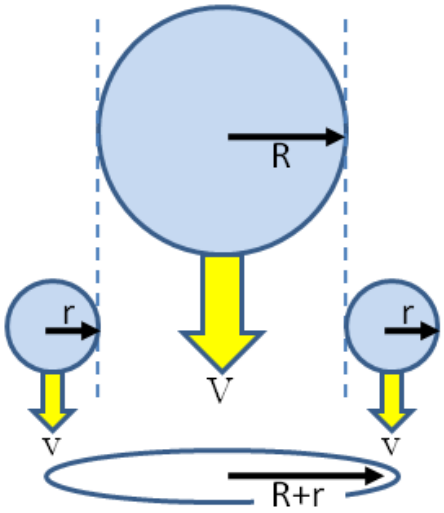

Figure 1.19: Schematic of collision and coalescence. Larger drops of radius R fall at terminal velocity V, collecting all smaller droplets of radius r within a cylinder of radius $R + r$.

recall states $\frac{dM}{dt} = 4\pi R^2 \rho_L \frac{dr}{dt}$ to give

$$\frac{dR}{dt} = \frac{LV}{4\rho_L} \tag{1.28}$$

If we take the case of the initial growth of small droplets ($r < 30$ μm) then the terminal velocity was given by $V = X_1 R^2$ giving

$$\frac{dR}{dt} = \frac{LX_1 R^2}{4\rho_L} \tag{1.29}$$

Thus the growth rate due to collisions is proportional to the square of the droplet radius in this regime, while we recall that the radius rate change due to the diffusive process was proportional to the inverse of radius. This implies that there is a changing balance between the competition of these two processes, with the dominance of diffusion overcome by the importance of the collection process as the radius increases (see 1.20)

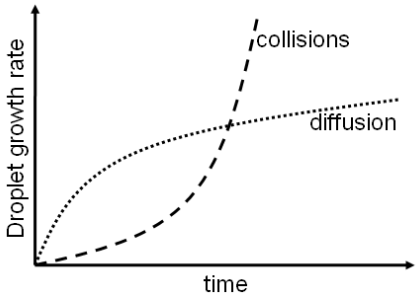

Figure 1.20: Schematic of droplet radius as a function of time resulting from growth by diffusion and collisions processes. NOTE: Y-AXIS LABLE IS INCORRECT AND SHOULD READ "DROPLET RADIUS", FIGURE WILL BE CORRECTED SHORTLY.

We can simply integrate (1.29) to show that for $L = 10^{-3}$ kg m^{-3} a drop can grow from 20 to 30 μm in approximately 10 minutes. We then need to introduce the relationship $V_t = X_2 R$ into (1.28) and integrate to calculate that the raindrop can attain a radius of around 300 μm in 20 minutes.

These times appear to be reasonable compared to cloud lifetimes, but we have ignored two effects in this simple view, *Q: Can you think what they might be?* We assumed simplistically that all droplets with in the large droplet trajectory collided with the large drop and that all collisions led to coalescence. Neither of these two assumptions are very accurate.

Collection efficiency $E(R, r)$

We saw earlier in Fig. 1.16 how the streamlines around various raindrop sizes looked. The lack of inertia of very small droplets implies that they will tend to get swept around the larger droplets if r/R is small (see Fig. 1.21). To describe this we introduce the *collision efficiency parameter* $E(R, r)$. For small r/R, $E(R, r)$ can be as low as 0.1, while when $R \sim r$ the flow fields can interact in a complex way and result in $E(R, r) > 1$.

Coalescence efficiency, ϵ

The *Coalescence efficiency* ϵ is often assumed to be $\sim$1, but observations show that it can be lower than 0.5.

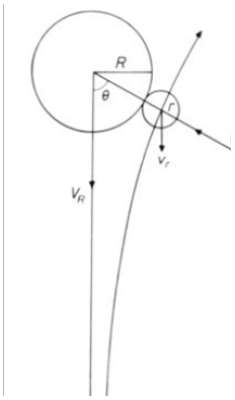

Figure 1.21: Schematic showing more realistic path of small droplet (source Mason, 1978).

Figure 1.22 shows two methodologies for the calculation of $E(R, r)$ from Klett and Davis (1973) which differ greatly for $R < 30$ μm in this case. Taking the *collision efficiency* and *Coalescence efficiency* into account modifies our radius growth rate equation to

$$\frac{dR}{dt} = \frac{LV\epsilon E(R, r)}{4\rho_L} \tag{1.30}$$

and growing a droplet from 20 to 30 μm can now take as much as *100 minutes* instead of 10 minutes, and we no longer grow rain drops in the observed time of cloud development. There are a number of mechanisms that lead to an accelerated growth rate to get us out of this impassé:

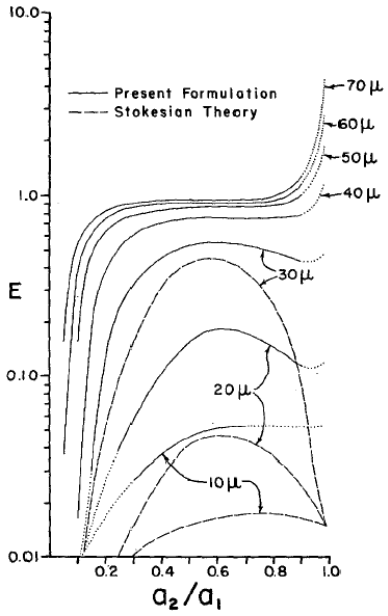

Figure 1.22: Graph of theoretical collection efficiencies $E(R, r)$ for two calculation methodologies with the x-axis showing the radii ratio r/R. Each line is labled with the radius of the larger droplet (source Klett and Davis, 1973).

- *Statistical models of raindrop growth*: we assumed that droplet growth was a discrete function of time, whereas it consists of a serious of discrete events. If in a time Δt 10% of raindrops collide and coalesce then after time $2\Delta t$ there will be one large drop from 100 initial droplets (see Fig. 1.23). But this larger droplet will then be favoured for further growth as the growth rate is $\propto r^2$. *A spectrum of drop sizes, often bimodal, is therefore generated* (see Fig. 1.24).
- It was also assumed that droplets were evenly distributed within the cloud, whereas in reality cloud are *inhomogeneous*, and regions of higher liquid water content will favour droplet growth.
- The process of *entrainment* cause the partial evaporation of droplets broadening the droplet size distribution.

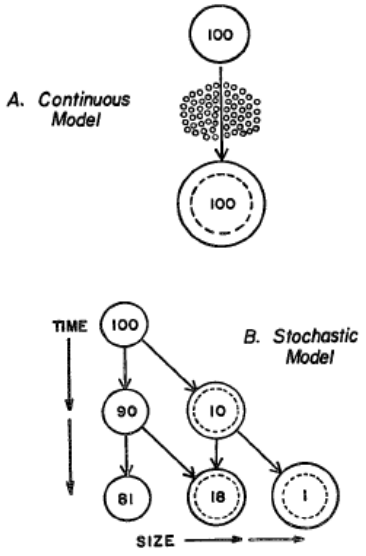

Figure 1.23: stochastic model of sweep out (source Berry, 1967).

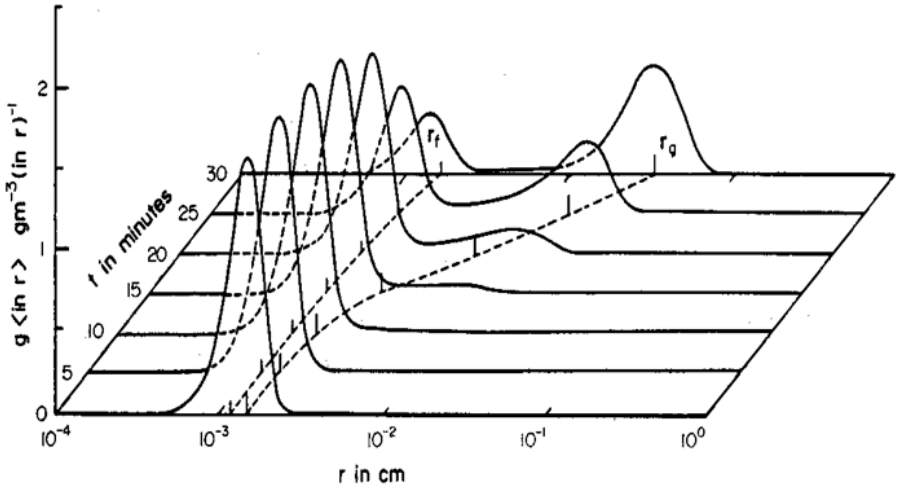

Figure 1.24: Example of the development of a droplet spectrum by stochastic coalescence (source Berry and Reinhardt, 1974).

Raindrop size distributions

In many parts of the globe frozen precipitate melt before they reach the surface and thus precipitation reaches the surface in the form of rain. There is a natural limit to the raindrop size due to droplet breakup, and it is usually very rare to measure raindrops with radii larger than 3mm - with 2mm a more common limit.

Q: If you stand underneath a tree during a shower, you may get much larger drops fall on you. Why?

The reduction in occurrence with droplet size implies that raindrop radii (or diameters) tend to follow an inverse exponential distribution, known as the Marshall-Palmer distribution (Marshall and Palmer, 1948), after the first authors to suggest the relationship from observations

$$N(D) = N_0 e^{-\Lambda D}, \tag{1.31}$$

where $N(D)dD$ is the number of drops per unit volume with diameters between D and $D + \Delta D$.

The slope factor *Lambda* depends on rainfall rate R and is given by

Q: what properties do you notice from the rainfall size distribution?

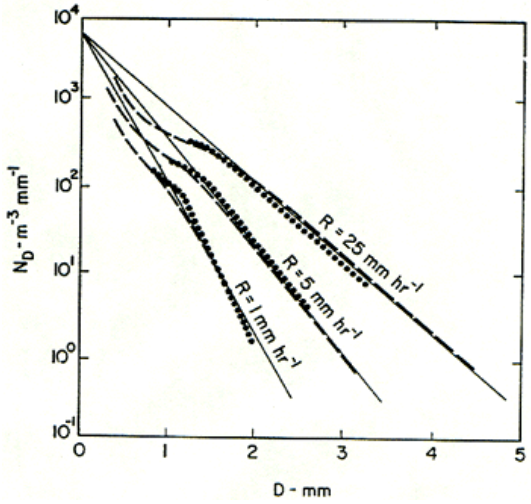

Figure 1.25: Marshall-Palmer distributions (from Marshall and Palmer, 1948)

$$-\Lambda(R) = 41 R^{-0.21}, \tag{1.32}$$

where the units of R and *Lambda* are mm hour^{-1} and cm^{-1}, respectively. It was also found that N_0 was independent of rainfall rate, taking a value of $N_0 = 0.08$ cm^{-4}. Fig 1.25 shows the Marshall-Palmer distribution.

Of course, these relationships are empirical and valid over a large-number of observations. Exact relationships will vary with location and time and departures from the MP distribution will always occur (Fig. 1.26).

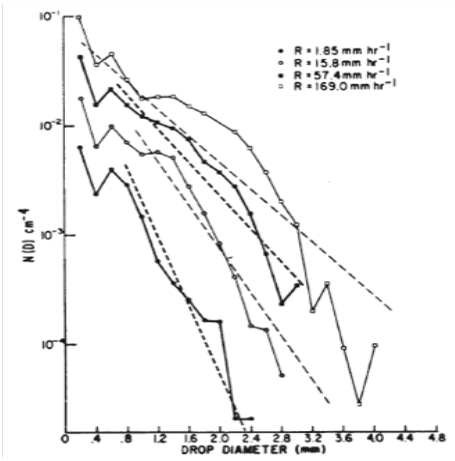

Figure 1.26: An example of raindrop size distributions from Willis (1984)

1.6 Ice crystal nucleation

Introduction to ice processes

The first thing that should be emphasized when considering the ice phase is that *ice phase processes in clouds are far more complicated (Fig. 1.27) and consequentially poorly understood* relative to the warm phase cloud processes. This course can only skim the surface of the relevant mechanisms.

Figure 1.27: Example of an ice crystal from http://www.its.caltech.edu/)

Liquid water was described as a state where water vapour molecules were jumbled together and weak hydrogen bonds were formed between molecules, which are constantly overcome by thermal agitation. If temperatures become low enough to prevent the disruptive effects of thermal motions, water freezes into ice in which the hydrogen bonds form a rigid and stable network (Fig. 1.28). In this well-defined structure of ice each water molecule is surrounded by four neighboring H2Os. Two of these are hydrogen-bonded to the oxygen atom on the central H2O molecule, and each of the two hydrogen atoms is similarly bonded to another neighboring water molecule. This lattice arrangement requires that the molecules be somewhat farther apart than would otherwise be the case in liquid and as a consequence, ice, in which hydrogen bonding is at its maximum, has a more open structure, and thus a lower density than water (Fig. 1.29).

1.7 Ice saturation

Saturation over a plane surface of pure ice

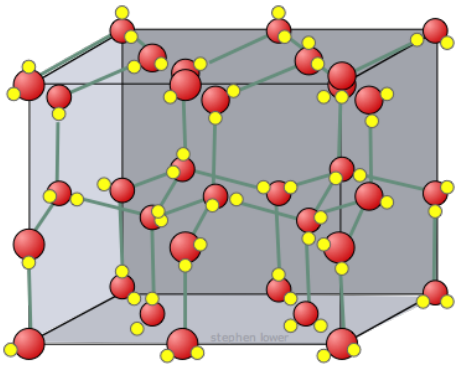

Figure 1.28: The ice latice structure (www.chem1.com)

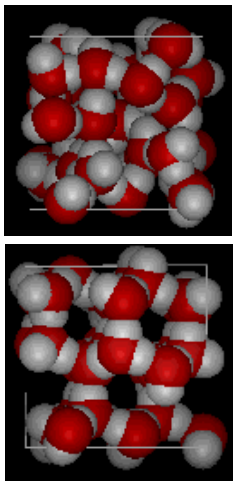

(a)

(b)

Figure 1.29: Schematic of (a) liquid and (b) ice molecular structures (source edinformatics.com)

Before we continue with the discussion of ice we must first consider the concept of saturation over a planar ice surface. Analogous to the liquid water saturation, the air is said to be saturated if the *deposition* (vapour→ice) rate equals the *sublimation* (ice→vapour) rate.

As the intermolecular bonding energy of molecules in ice is greater than that in liquid water, at a given temperature, the evaporation rate is larger than the sublimation rate. Thus it is clear that $e_{si}(T) < e_{sw}(T)$ (see Fig. 1.30) where the saturation vapour pressures are

- e_{si} over ice
- e_{sw} over liquid water.

Note that while the *ratio* $\frac{e_{sw}}{e_{si}}$ increases with decreasing temperature, the highly nonlinear saturation curves implies that this is not true of the *absolute difference* between the two $e_{sw} - e_{si}$, which reaches a maximum at a temperature of around -15^{o}C.

1.8 Ice nucleation mechanisms

There are three potential mechanisms by which ice clouds can form:

1. Homogeneous freezing from the liquid phase
2. Homogeneous nucleation from the vapour phase
3. Heterogeneous nucleation from the vapour phase

Homogeneous nucleation from the vapour phase (mechanism 2) requires very high relative humidities for similar reasons to those given for the warm phase, and thus this is not a viable mechanism

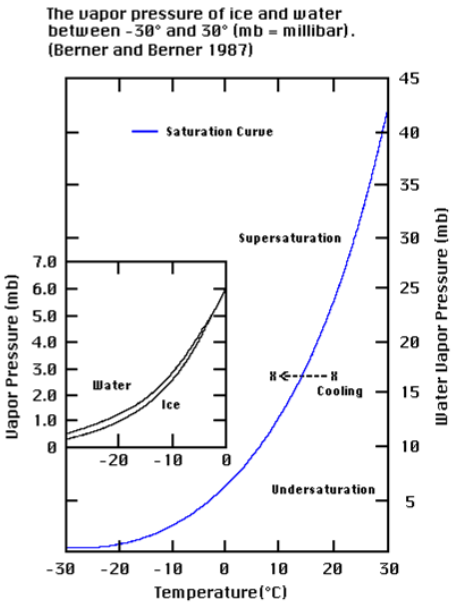

Figure 1.30: Water and ice saturation vapour pressures (from Berner and Berner 1987)

for ice crystal formation in the atmosphere. Thus the two key methods by which ice can form is by *freezing of a liquid droplet*, or by direct *vapour deposition on an ice nucleus* (heterogeneous deposition nucleation).

The balance between these two mechanisms depends on the *cloud updraught speed* and the *ambient temperature*.

- *Homogeneous* nucleation is often the dominant process in clouds forming at temperatures colder than -40C (cirrus) or clouds with fast updraught speeds,
- *Heterogenous* nucleation from the vapour phase may dominate crystal formation in mixed phase clouds at temperatures above -40C or also in clouds with slow vertical updraught speeds if sufficient IN are present

ICE2

1.9 Homogenous nucleation from the liquid phase

When the temperature falls below 0°C there is no guarantee that freezing of liquid cloud droplets will immediately occur. Freezing begins when an initial crystal, termed *ice germ*, is formed by statistical fluctuations of the liquid molecular arrangement to form a stable ice-like lattice structure. As in all nucleation processes, energy is required for the formation of the ice germ surface:

$$\Delta G_{i,w} = 4\pi r^2 \sigma_{i,w} - \frac{4\pi r^3 R_v T}{3v_i} ln \frac{e_{s,w}}{e_{s,i}} \tag{1.33}$$

Thus, the lower the temperature, the larger $\frac{e_{s,w}}{e_{s,i}}$ becomes, which lowers the energy barrier to form a critical ice germ. From Fig. 1.31 it is seen that at colder temperature the energy barrier is far lower than that for homogenous liquid or ice crystal nucleation from the vapour phase. If the germ is over a critical size, then other water molecules will bind to the ice germ rapidly and the water body will freeze rapidly. Again, we refer to concepts of statistical mechanics. The larger a body, the more likely it is that random energy fluctuations will occur to create an ice germ of a critical size for spontaneous freezing to occur. Large drop are more likely to freeze than small drops. It is clear that a pond therefore freezes more readily than a cloud of liquid droplets as the formation of an ice germ of critical size only has to occur once in the pond, while the event needs to occur in each cloud droplet which is far less likely. Thus it is possible and indeed very common to find liquid cloud drops existing at temperatures much below the freezing point; referred to as *supercooled droplets* (see Fig. 1.32). Theoretical results imply that a liquid drop of 5 μm will

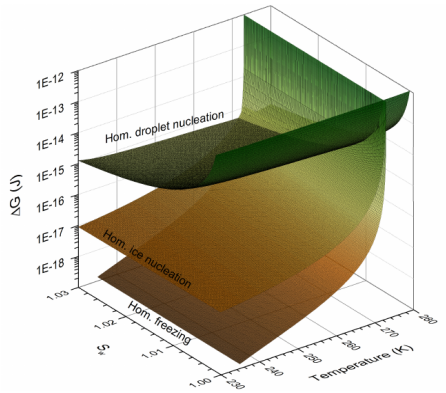

Figure 1.31: Gibbs free energy barrier for homogeous nucleation phase transitions (from Lohmann U.)

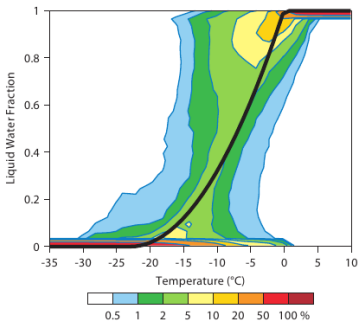

Figure 1.32: Liquid water to ice fraction in the ECMWF cloud scheme (Forbes et al. 2011).

spontaneously freeze at temperature of around -40°C, however, these calculations are uncertain as $\sigma_{i,w}$ is poorly known. Empirical measurements inside real clouds show that they contain no liquid drops once temperatures of around -35°C to -40°C are attained (depending on the cloud drop size spectra). Such clouds are said to be completely *glaciated*.

Homogeneous nucleation of ice from vapour

It is also theoretically possible to nucleate ice crystals directly from the vapour phase, however theory shows that very high supersaturations ($> 1000\%$) with respect to ice would be required. At these high supersaturations, air would also be supersaturated with respect to liquid water, forming droplets that would freeze. Thus *homogeneous nucleation of ice directly from the vapour phase is not a relevant mechanism* for creating ice cloud.

Ice supersaturation in the upper troposphere

One consequence of the lack of efficient IN is that cloud-free air can be supersaturated with respect to ice and not form ice cloud. However there is an upper limit to the amount of ice supersaturation set by e_{sw} since at this point liquid droplets form which will homogeneously freeze *if* the temperature is below -40°C. A common sign of the upper troposphere being supersaturated is the presence of *permanent contrail cloud* (Fig. 1.33).

As temperature get colder, e_{sw} and e_{si} diverge, and larger ice supersaturations are possible. In fact it is more complicated and the limit is below e_{sw} since we recall that aqueous solution droplets (haze) forms at RH with respect to water substantially below 100%.

Koop et al. (2000) investigates this limit in detail and shows an upper limit of 45% ice supersaturation at $T = 235$ K increasing to 67% at $T = 190$K.

In Fig. 1.34 Spichtinger et al. (2003) shows using retrievals from microwave limb sounder data that ice supersaturated states are quite common in the upper troposphere. We have seen that homogeneous ice nucleation occurs at temperature below -40°C and that supercooled liquid water is very common below 0°C. However it is also true that ice is observed in clouds between 0°C and -40°C. Clouds *Q: How could it get there?*.

Figure 1.33: Photo and satellite picture of permanent contrails over the UK. (source unknown).

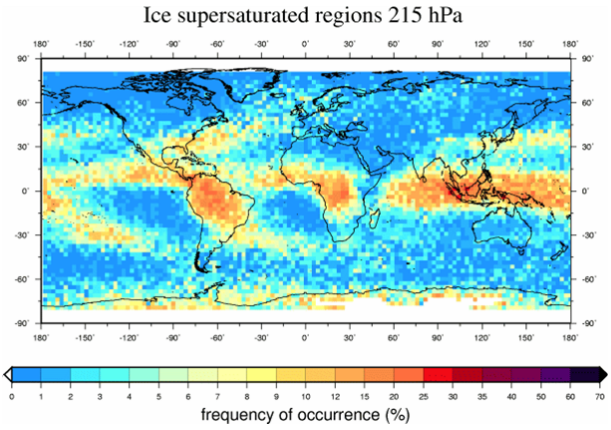

Figure 1.34: Frequency of ice supersaturation at 215hPa (source Spichtinger et al., 2003)

- Air was previously at much colder temperatures: *parcel history*
- Ice has fallen from above: *ice sedimentation*
- Ice has nucleated in situ: *how?*

Ice can form by collision of liquid water droplets with other ice crystals, freezing on contact. Alternatively, ice crystals can form with the aid of aerosols in a heterogeneous nucleation process. ICE3

Heterogeneous nucleation of ice

Aerosols in the atmosphere can also act as *ice nuclei* (IN) if their molecular structure is close enough to the lattice structure of ice. The first point to emphasize is that it is much less common for aerosols to have this property and therefore ice nuclei are much less common than CCN.

At $T = -20°\text{C}$ a typical number concentration (NC) of ice nuclei might be 10^{-3} cm^{-3} compared to CCN of roughly 10^{2} cm^{-3}.

Whether an aerosol can act as a cloud nuclei depends on the *ice supersaturation* and the *temperature*.

As ice supersaturation increases and temperature reduces more aerosols take on the property of being ice nuclei. Fletcher (1962) found that for each 4°C of cooling the number of ice nuclei increases by a factor of ten (Fig. 1.35).

Common ice nuclei

Some ice nuclei are given in table 1.3 along with their maximum nucleation temperature.

Demott et al. (2003) tested air samples taken from mountain top in mid-Western USA and documented the distribution of IN depicted in Fig. 1.36. The wide range of supersaturation and temperature thresholds for various classes of IN is shown in Fig. 1.37 which is taken from Hoose and Möhler (2012). It should be emphasized that knowledge of which aerosols can act as ice nuclei is uncertain and the subject of current research. Ice nuclei concentrations are highly variable, and although the Fletcher curve may be accepted as typical, concentrations can vary by orders of magnitude. Aerosols may also be carried a long distance in the atmosphere before being

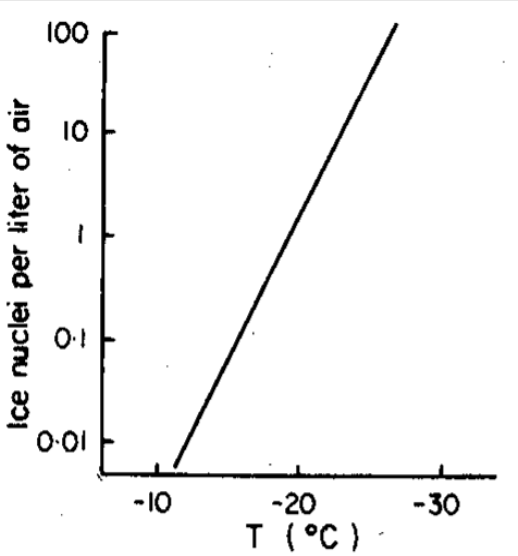

Figure 1.35: Ice nuclei concentration as a function of temperature (source Fletcher, 1962)

Substance	Nucleation T (°C)	Notes
ice	0	
silver iodide	-4	used in cloud seeding
clay	-9	often seen in snow crystals
cholesterol	-2	
bacteria(!)	close to 0	used in snow machines

Table 1.3: ice nuclei and their nucleation temperature maximum

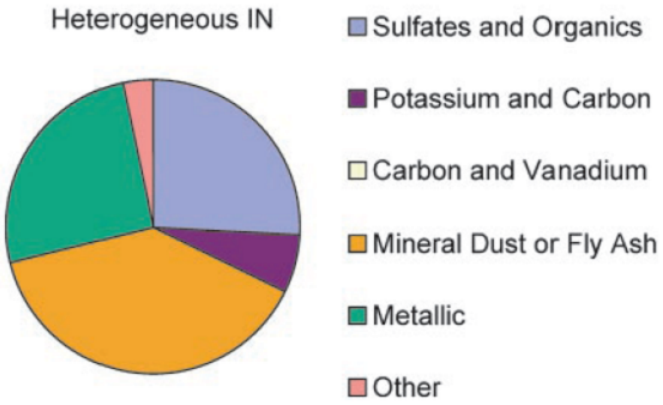

Figure 1.36: From Demott et al. (2003), distribution of IN type from air samples taken over the mid-West USA.

involved in ice cloud nucleation events. Demott et al. (2003) and others have shown that mineral aerosols from Western Africa are a significant source of ice cloud nuclei over the United States for example! In fact many snow or ice particles contain clay mineral aerosols indicating that the desert regions of the world are in general an important source of IN (see Fig. 1.38). ICE3

General properties of ice nuclei
Observations and laboratory experiments indicate that aerosol particles usually satisfy a list of criteria if they are to serve as IN (Pruppacher and Klett, 1997).

- **Insolubility criterion:** In general, IN must be very insoluble. The disadvantage of a soluble substrate is that it disintegrates under the action of water. Hence the molecular structural requirement for ice nucleation can not be maintained.

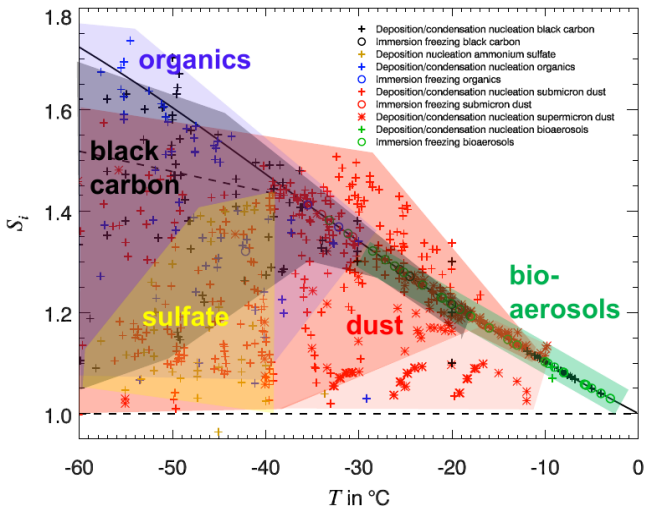

Figure 1.37: The onset temperatures and relative humidities for IN from a compilation of experimental data of sub- and supermi- cron aerosol particles in the literature from Hoose and Möhler (2012). The wide variability in the thresholds is emphasized.

What kind of cloud is this figure showing?

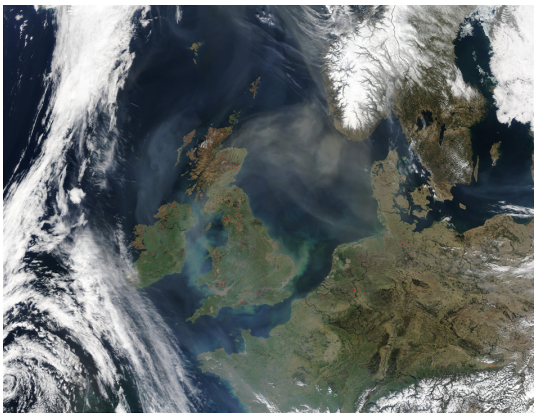

Figure 1.38: Modis image over Europe (source MODIS website)

- **Size criterion:** IN must have a size comparable to, or larger than, that of a critical ice embryo. Generally speaking the radius of the IN must be greater than 0.1 μm; i.e. Aitken particles do not tend to be ice nuclei. At sizes less than this critical radius (0.1 μm), the nucleating ability of the particle decreases rapidly (and becomes increasingly more temperature dependent).

- **Chemical Bond criterion:** The chemical nature of an IN, that is the type and strength of the chemical bonding sites at the IN surface, affect nucleation. In view of this bond criterion, certain complex organic molecules (i.e. aerobic bacteria) exhibit good ice nucleation abilities. The hydrogen bonding groups in ice are similar to the hydrogen bonding groups in many organic molecules.

- **Crystallographic criterion:** Since ice nucleation on a substrate is actually an overgrowth of ice on the substrate, it is reasonable to expect the nucleating ability of the substrate to increase when the lattice structure of the substrate is similar to the hexagonal lattice structure of ice. In this way, molecular matching between the molecules of ice and the substrate may be achieved (Fig. 1.39). The crystallographic matching reduces the *"misfit"* and *elastic strain* in the ice.

Both of the properties of misfit and elastic strain reduce the nucleating ability of the substrate. Kaolinite forms good ice nuclei because it has a *pseudo-hexagonal structure*. AgI (silver iodide)

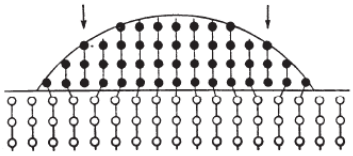

Figure 1.39: An ice-embryo (dark points) growing upon a crystalline substrate with a misfit of 10%. The interface is dislocated, dislocations being indicated by arrows. (from Fletcher, 1969) **?**.

also has a hexagonal form. Other molecules have a non-hexagonal shape (e.g. cubic), but still have crystal structures close enough to ice to aid nucleation. The crystallographic requirement has to do with the arrangement of molecules and is distinct from the chemical bond criterion.

- **Active Site criterion:** Ice nucleation generally occurs at distinct sites on the substrate. Laboratory studies have indicated that ice nucleation is preferred on those substrates which have pits and steps on their surfaces. Those nuclei that have smooth surfaces are less efficient nuclei, that is, nucleation occurs at *lower temperatures*. An example is shown in Fig. 1.40 where ice crystals preferentially formed on steps etched onto the surface of a cadmium iodide crystal.

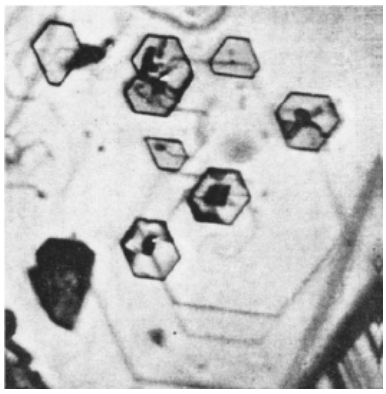

Figure 1.40: An epitaxial deposit of ice crystals growing at the steps of a hexagonal growth spiral on cadmium iodide (source **?**).

Mechanisms for Heterogeneous Nucleation

There are several mechanisms for ice crystal nucleation, schematically illustrated in Fig. 1.41.

These are

- heterogeneous deposition nucleation: the vapour undergoes deposition directly onto the IN
- condensation nucleation: the IN acts first as a CCN to form a liquid droplet, and then acts as a IN to initiate freezing
- contact nucleation: a supercooled liquid droplet undergoes freezing immediately on contact with the IN
- immersion nucleation: IN absorbed into a liquid droplet, and later initiates freezing event, possibly after droplet cooling.

ICE4 Contact freezing and immersion freezing occur in mixed phase clouds in which the ambient vapour pressure is equal to the saturation vapour pressure with respect to liquid water. *Why?*

The deposition of water vapour directly onto IN can occur at saturations substantially less than water saturation. Fig. 1.42 the pathways for ice nucleation are shown, along with the threshold for homogeneous ice nucleation.

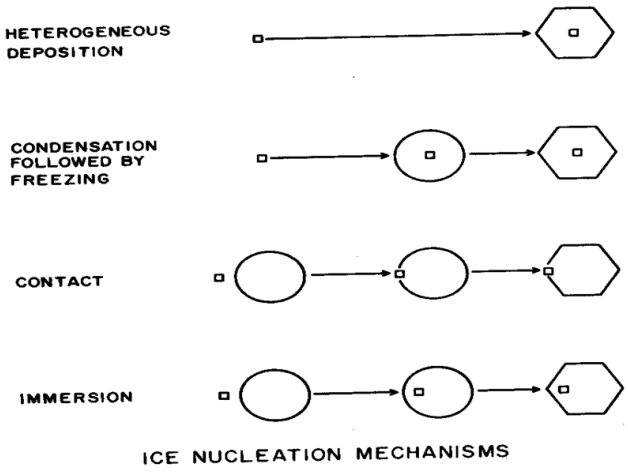

Figure 1.41: Schematic of heterogeneous nucleation pathways (source: Rogers and Yau, 1989).

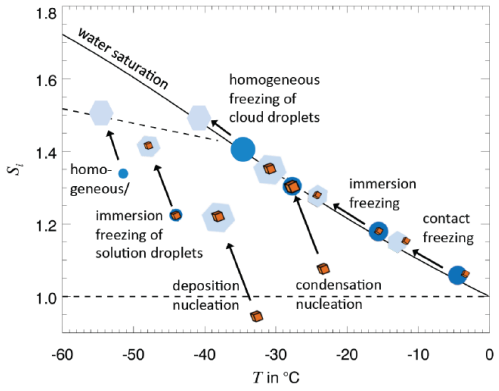

Figure 1.42: Atmospheric trajectories of temperature and ice saturation of a rising air parcel which lead to ice formation in the different nucleation modes (source Hoose and Möhler, 2012)

1.10 Ice crystal growth

We divide the consideration of ice crystal growth by diffusion of water vapour into two regimes: *mixed phase* and *glaciated* clouds. For *mixed phase clouds* we recall that at subfreezing temperatures the ice and water vapour saturation pressures diverge, and thus an air volume at water saturation is supersaturated with respect to a planar ice surface, reiterated in Fig. 1.43.

Bergeron-Findeison Effect
The *Bergeron-Findeison effect* is an important growth enhancing mechanism in mixed phase clouds. In a supercooled liquid water cloud imagine one liquid droplet freezes (Fig. 1.44):

- The cloud is initially saturated *with respect to liquid water*.
- It is thus *ice* supersaturated.
- The ice crystal will grow by diffusion of water vapour towards the crystal,
- This reduces the vapour pressure below the liquid water saturation value.
- The liquid droplets evaporate on a fast timescale maintaining the vapour pressure close to the liquid water saturation.

The outcome of the Bergeron-Findeison effect is that the growth rate of the ice crystal is faster than it would be in the absence of liquid cloud droplets. For a water saturated environment the growth rate is fastest when the difference between the saturation limits is largest *in absolute (not relative!) terms*. This occurs around $T = -15°\mathrm{C}$.

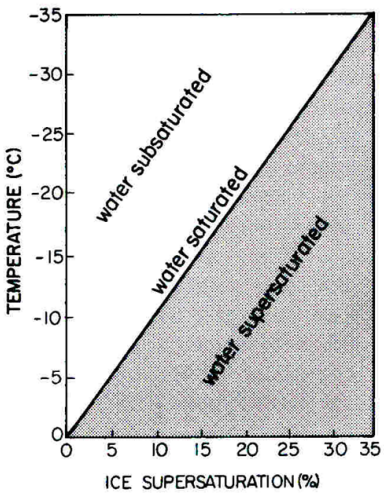

Figure 1.43: Diagram showing relative degrees of ice and liquid water super or sub-saturation as a function of temperature (source: Pruppacher and Klett, 1997))

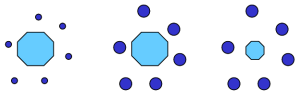

Figure 1.44: Schematic of Bergeron-Findeison process, with the cyan hexagon representing an ice crystal in a liquid water cloud

A laboratory photo shows the result of the BF-effect, with the lack of liquid droplets surrounding the ice crystal on the plate (Fig. 1.45)

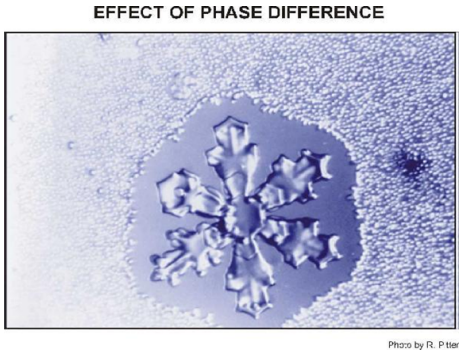

Figure 1.45: Photo of BF-Effect (source R. Potter from ?)

Ice Habits

Ice habits can be very complex and depend on the temperature and ambient ice supersaturation at which ice nucleation takes place (Fig 1.46). The crystal shape has a strong impact on radiative properties (Macke et al., 1996) and the fall speeds of the ice particle.

Ice forms crystals having a hexagonal lattice structure, which in their full development would tend to form hexagonal prisms very similar to those sometimes seen in quartz. This does occasionally happen and depends on the ambient temperature and supersaturation. More commonly, crystals form in a flattened fractal-like hexagonal structure. Ice that grows under warmer conditions grow more slowly, resulting in smoother, less intricate shapes. A classification of ice shapes in shown in Figure 1.47.

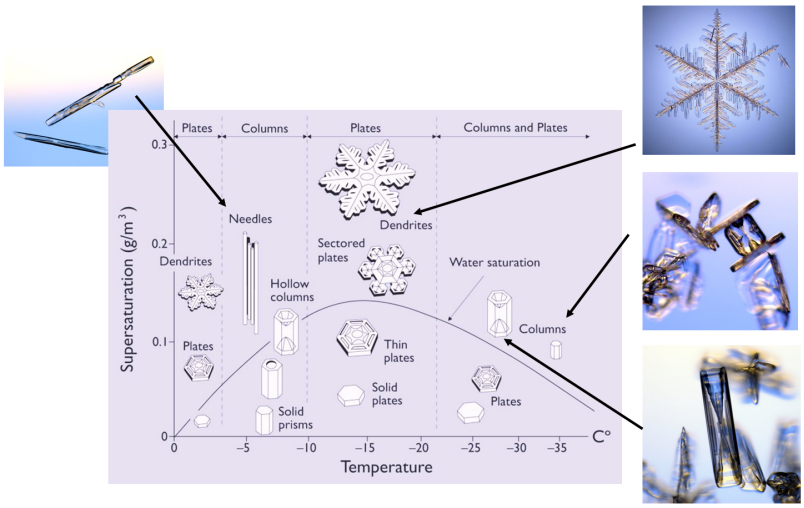

Figure 1.46: Ice crystal types as a function of S_i and T (source caltech.edu)

Figure 1.47: Ice crystal categorization (source caltech.edu)

1.11 Competition between ice nucleation mechanisms

Competition between ice nucleation mechanisms
At temperatures warmer than -40°C the only nucleation mechanism is heterogeneous. However at temperatures colder than this both heterogeneous and homogeneous nucleation can occur contemporaneously.

As many IN become active at ice supersaturations of 10 to 30%, well below the threshold range for homogeneous nucleation, then homogeneous nucleation has the potential to be the dominant nucleation mechanism, *if and only if* IN are present in sufficient numbers to prevent the RH reaching the homogeneous nucleation threshold in a rising (cooling) parcel of air.

Q: Both mechanism create ice crystals, so why do we care which one dominates? Demott et al. (2003) (Fig. 1.48) documents the concentration of nucleated ice crystals as a function of water saturation for air samples collected over the western United States. For $T > -35°C$ the NC increases with supersaturation as more aerosols become active. However at cold temperatures there is a step jump close to water saturation to much higher concentrations due to homogeneous nucleation. . *Homogeneous nucleation thus has the potential to create a much higher concentration of cloud ice crystals - Q: Why?* The homogeneous nucleation process creates more ice particles since it is due to the freezing of aqueous solution droplets and thus related to the number of CCN. The particles nucleated by homogeneous process are much smaller in size therefore.

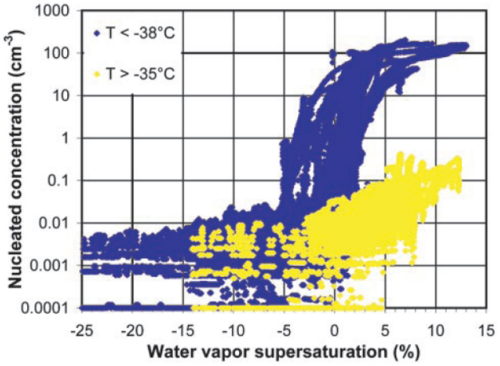

Figure 1.48: Nucleated ice crystal number in air samples as a function of water saturation at two temperatures. (source: Demott et al., 2003).

Whereas in warm clouds the droplet concentration was related directly to the CCN number, in ice clouds the relationship between IN and ice particle number concentration is more complicated and nonlinear, falling into two distinct regimes, illustrated schematically in Fig 1.49. The figure shows three cases of an lifted hypothetical parcel of air at cold temperature ($T < -40°C$). The left case is for a clean sample of air with no IN. The parcel rises until the RH attains the threshold for homogeneous nucleation, 160% in this example. Many ice particles ensue. These rapidly grow by depositional growth as the air is highly ice supersaturated and the water vapour content returns rapidly (in seconds to minutes) to the ice saturation vapour pressure.

The middle column shows a parcel of air with a low number of IN. These nucleate ice at lower supersaturation thresholds (say 30%) but the number is too small to "use up" (by deposition) much vapour and the homogeneous threshold is still reached. Nevertheless the "overshoot" over this threshold and number of aqueous particle formed will be less due to the take-up of vapour by the IN, and thus the final total number of ice crystals will be less. This also implies that the return of the vapour content to the ice saturation value will be slower.

Finally the right hand column shows air with a high enough content of IN such that the ice particles nucleated are sufficiently numerous to prevent the RH from even reaching the threshold for homogeneous nucleation and the latter mechanism is effectively inhibited. The final number of ice particles is orders of magnitude lower than in the clean air case and the return to ice saturation is much slower and may take on the order of an hour or longer.

After this point further increases of IN will increase the ice particle concentrations as in warm phase clouds, but always at much lower concentrations than produced by homogeneous nucleation.

The final number of ice crystals will be dependent on the both the IN concentration of the air and the updraught velocity of the air parcel. As in warm clouds, parcel models are used to study this, as in this example of Ren and Mackenzie (2005) in Fig.1.50. *In a weather or climate model, what are the issues involved in representing this relationship?* The following points should be noted about the parcel model results in Fig.1.50:

- The *overshoot* past S_{cr} for homogeneous nucleation determines the *number* of ice crystal nucleated.
- The overshoot has a timescale of seconds, and thus is not temporarily resolved by numerical models (parcel models use sub-second timesteps to resolve this),

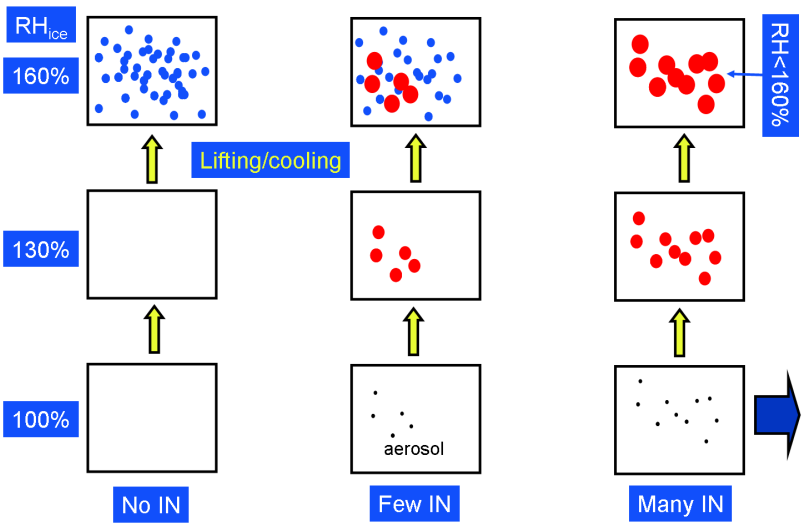

Figure 1.49: Schematic of homogeneous and heterogeneous nucleation competition, see text and lesson for details

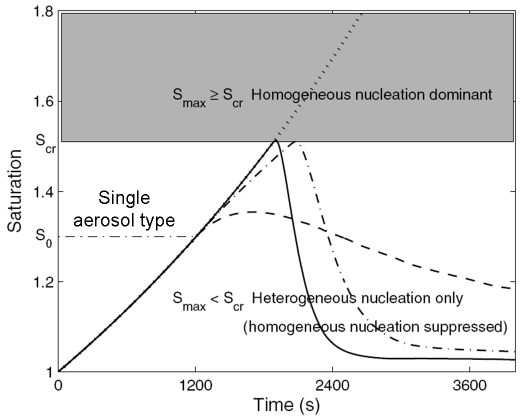

Figure 1.50: Results from parcel model of Ren and Mackenzie (2005) using a single aerosol type with a IN property threshold of $S = 1.3$

- The overshoot depends on the updraught velocity and also the number of aerosols present and their own nucleation (S_{cr}) properties.
- A numerical model needs to be able to resolve the updraught velocity of the parcel *on the scale of the cloud*
- A numerical model needs to have accurate information concerning the aerosol quantities present.
- In many cases the diffusional growth timescale is also less than the timestep of a typical global model (O(1 hour)).

Another example of this work is Gierens (2003). To pick up on the point concerning the model vertical velocity, Fig. 1.51 gives typical PDFs observed and also modelled using a global model. It is seen that the coarse resolution of the model truncates the spectra and does not resolve the highest velocities occurring on small spatial scales. Some success at reproducing the statistics of the vertical velocity spectrum is achieved with a simple parametrization.

In (Tompkins et al., 2007), I attempted to implement a modified cloud scheme into a weather forecast model that takes the zero-order effect of the elevated homogeneous nucleation threshold into account. The schematic in 1.52 shows the RH evolution of a air parcel undergoing homogeneous nucleation and model assumptions the dotted line add shows the assumptions made in

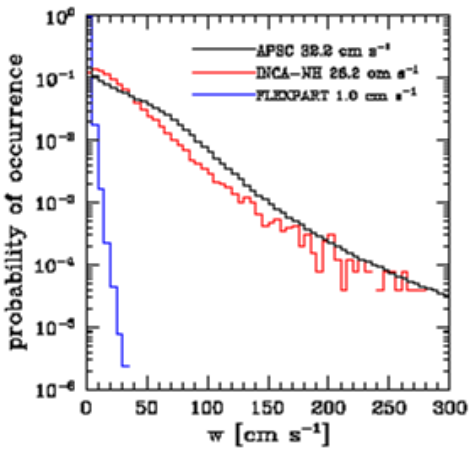

Figure 1.51: Results from Lohmann (citation needed) showing PDF of vertical velocity from (blue) a global model (red) aircraft observations and (black) model results corrected with a simple turbulence based parameterization for use in a ice-cloud model.

many models (middle panel) and the new scheme (right). The new scheme allows the clear air to be supersaturated, but assumes that once ice crystals are nucleated they grow instantaneously by diffusion to return the vapour to ice saturation within a model timestep. The *zero order* effect of the ice nucleation threshold and *hysteresis* behaviour is captured.

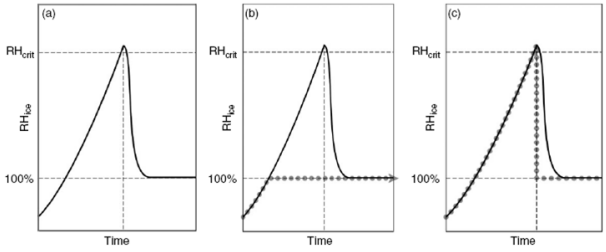

Figure 1.52: Schematic from Tompkins et al. (2007) showing (left) the *RH* evolution of a air parcel undergoing homogeneous nucleation and model assumptions.

Such a simple scheme is able to reproduce the distribution of frequency of occurrence of supersaturation from satellite retrievals and the PDF of *RH* from aircraft well (Fig. 1.53).

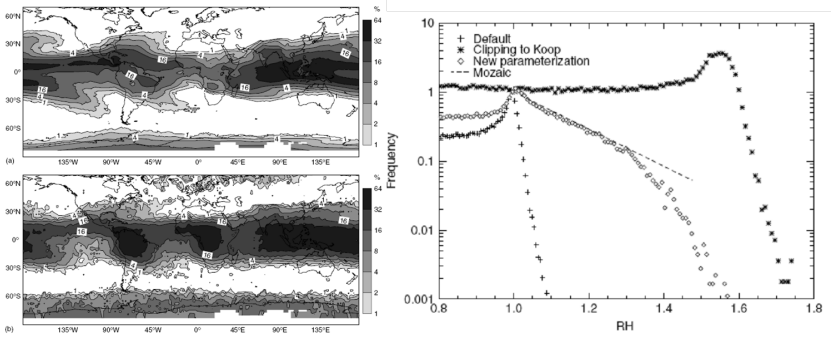

Figure 1.53: Results from Tompkins et al. (2007) showing (left) freq of occurrence of supersaturation compared to retrievals of Spichtinger et al. (2003) and (right) PDF of *RH* compared to Mozaic data of Gierens et al. (1999)

Some final thoughts

Errors in the map reflect errors in the convection occurrence in this version of the model known from other sources. We note

- that model error sources may be remote and are not easy to track down (cancellation of errors) and
- parametrization complexity does not need to exceed that necessary to represent the zero-order effect of the process, your knowledge of the process, or the complexity of the models' other components!

1.12 Aggregation

Aggregation
The ice particle that form from diffusional growth from an ice crystal are called *pristine*. However pristine ice particles can clump together to form *snowflakes* in a process known as *aggregation*.

At temperatures as low as 200K, the surface of ice is highly disordered and water-like. As the temperature approaches the freezing point, this region of disorder extends farther down from the surface and acts as a lubricant.

Thus the efficiency of the aggregation process increases as the temperature exceeds -5°C, when ice surfaces becomes *sticky*. There is also a secondary peak between -10°C and -16°C when dendrite arms get entangled. Figures 1.54 and 1.55 show example aggregates of bullet rosettes and other aggregates.

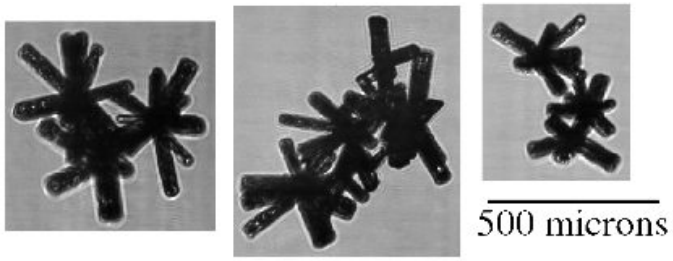

Figure 1.54: Bullet Rosette aggregates aggregates (source Dr. Chris Westbrook, Reading University, UK)

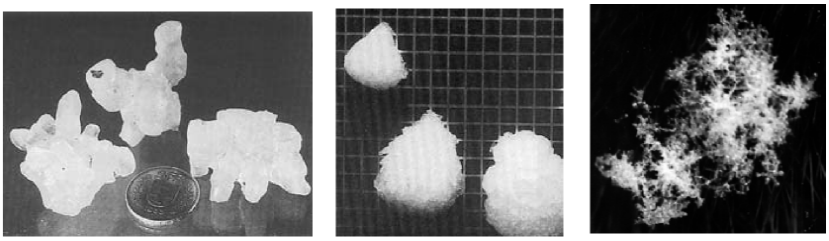

Figure 1.55: Other aggregate example (source Eszter Barthazy).

1.13 Riming

Riming to form graupel
If vapour exceeds the water saturation mixing ratio (in strong updraughts) then water can condense on ice crystals, and then subsequently freeze to form *graupel*, which are round ice crystals of higher densities.

Graupel and Hail are also formed by aggregating liquid drops in mixed phase clouds (see schematic in Fig. 1.56).

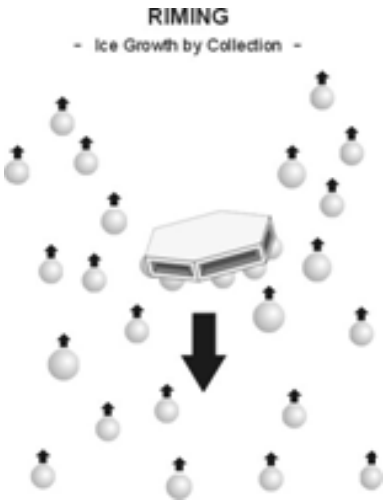

Figure 1.56: Schematic of riming process (source unknown)

Some examples of lightly and heavily rimed ice are given in Fig. 1.57. If the latent heat of condensation and fusion keeps temperature close to 273K then high density *hail* particles can form, since the liquid water *"spreads out"* before freezing. Hail is dense and thus has high terminal velocities (up to 40 m/s) implying that it only forms in convection with strong updraught able to support the particle long enough for growth

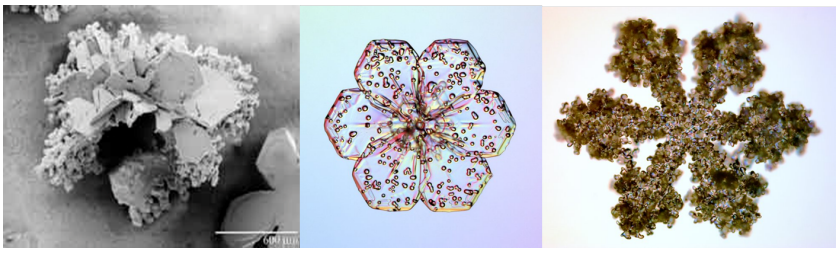

Figure 1.57: Photos of lightly and heavily rimed ice (source caltech.edu)

1.14 Ice particle fall-speeds

The density and size of ice particles determines their respective fallspeeds and its dependence on particle radius (Fig. 1.58).

There are implications for numerical models that may become clear examining radar animations of cloud systems (see link). *can you think what these might be?*

1.15 Ice multiplication

Ice multiplication

In recent years it has become increasingly evident that concentrations of ice crystals in "real" clouds are not always represented by the concentrations of IN measured or expected to be activated in such environments. In particular, it has been found that at temperatures warmer than -10°C the concentration of ice crystals can exceed the concentration of IN activated at cloud top temperature by as much as three or four orders of magnitude

There have been a number of hypotheses which have been advocated to explain such discrepancies. In particular, these hypotheses attempt to account for the unexpectedly high concentrations at warm temperatures. Some of the leading hypotheses are:

1. Fragmentation of large drops during freezing.

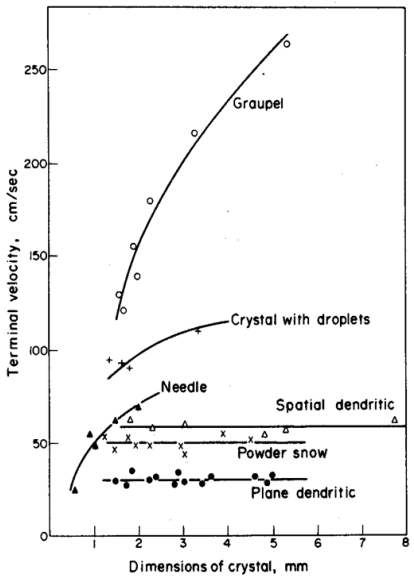

Figure 1.58: Fallspeeds of bulk ice particle categories (source: Rogers and Yau, 1989).

2. Mechanical fracture of fragile ice crystals (i.e., dendrites and needles) caused by collision of these crystals with graupel and other ice particles.

3. Splinter formation during riming of ice crystals.

4. Artificial measurement artifact of ice crystals shattering on impact with aircraft measurement device inlet.

Aircraft observations of ice in mid-level clouds observed in aircraft campaigns by Fleishauer et al. (2002) are shown in Fig. 1.59. Although many models make simple assumptions such that ice particle size reduces with temperature, it is seen that this is not necessarily valid in clouds with strong mixing. The small particles may only appear circular due to instrument resolution limitations.

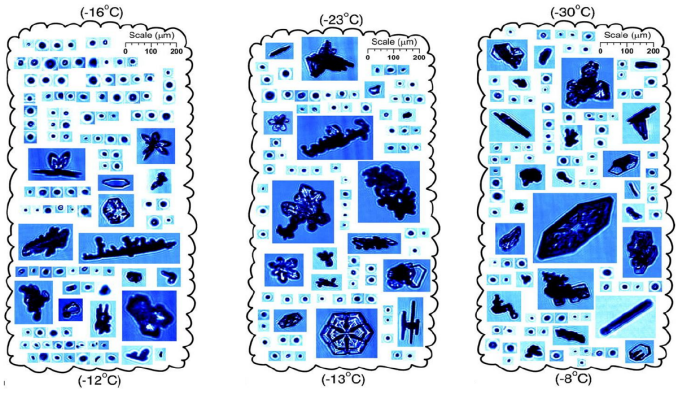

Figure 1.59: Example ice crystals from aircraft observations in mid-level cloud systems by Fleishauer et al. 2002 Fleishauer et al. (2002).

Snowflake size distributions

Most of the ice precipitation that reaches the ground does so as snowflakes and not pristine ice crystals.

Since snowflakes are irregular aggregates of crystals there is no simple way to measure their dimensions, thus they are usually measured in terms of their mass or, equivalently, the diameter of the water drop that would form from their melting.

Gunn and Marshall (1958) found that the exponential approximation still fits the snowflake

diameter well with the following parameters:

$$-\Lambda(R) = 25.5R^{-0.48}, \tag{1.34}$$

and

$$N_0 = 3.8 \times 10^{-2} R^{-0.87} \tag{1.35}$$

where the units of R and *Lambda* are mm hour^{-1} and cm^{-1} (Fig 1.60). To summarize, the key

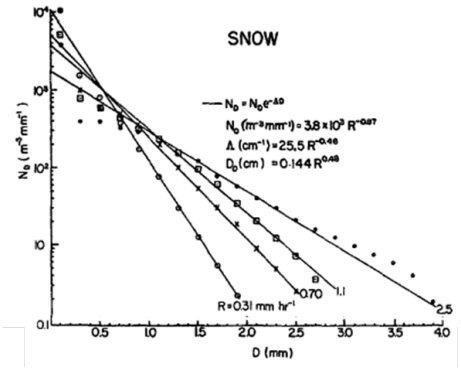

Figure 1.60: Snow flake size distributions (from Gunn and Marshall, 1958)

growth mechanisms are summarized in Fig. 1.61. and the location of some of these key processes

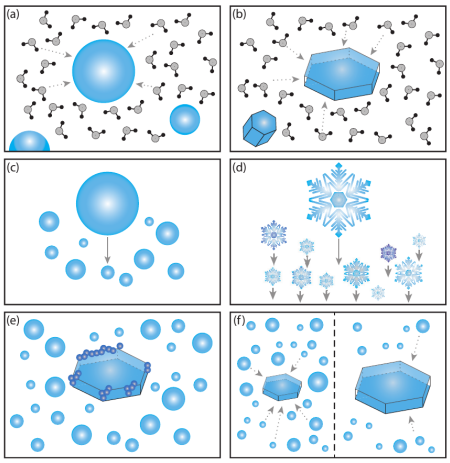

Figure 1.61: Crystal growth processes (a) condensation (b)deposition (c)collision-coalescence, (d) aggregation, (e) riming, (f) Bergeron-Findeisen process. (from Lohmann, U.)

in a typical deep convective cloud are given in Fig. 1.62.

Reminder Questions

- explain at the board what it means for an aqueous aerosol solution droplet to become "activated".
- What are the main mechanisms of ice nucleation that are relevant for ice cloud formation?
- How is a cloud called that consists only of ice, and one which consists of both liquid and ice? In roughly which temperature regimes does each cloud type exist? In the mixed phase explain what the Bergeron-Findeison effect is for ice growth
- Explain why we can find air that is supersaturated with respect to ice but not with respect to liquid water? What kind of cloud is an indication of supersaturated layers?
- Does the liquid cloud droplet radius increase or decrease with CCN number? Assuming that in a forming cloud, condensing liquid water is equally distributed among CCN, write down the relationship between droplet radius and cloud liquid water density in kgm^{-3}

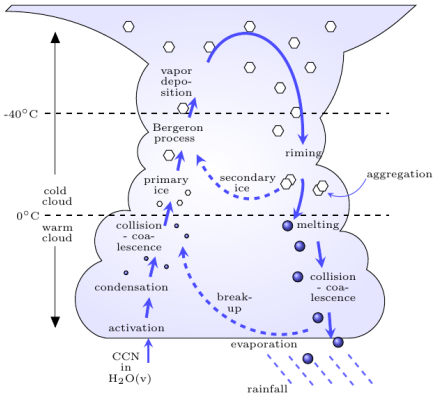

Figure 1.62: microphysical processes in a deep convective cloud (from Lohmann, U.)

- Does the ice crystal radius increase or decrease with ice nuclei (IN) number? What is a common source of IN?
- What are the two main mechanisms by which activated aerosols grow into raindrops, and under which droplet size radius do they operate and why? We made a number of approximations in our mathematical descriptions of the two processes, can you name some?
- What factor directly determines the number of ice crystals nucleated by each homogeneous nucleation, and what is this dependent on in turn?

Chapter 2

Tables

Table 2.1: Table of thermodynamical constants

Avogadro's constant	N_A	6.02×10^{23}	mol $^{-1}$
Specific heat capacity at constant pressure for dry air	c_p	1005	J kg^{-1} K^{-1}
Specific heat capacity at constant volume for dry air	c_v	718	J kg^{-1} K^{-1}
Ratio of gas constants	$\epsilon = \frac{R_d}{R_v}$	0.622	
Latent heat of vaporization	L_v	2.5×10^6	J kg^{-1}
Latent heat of sublimation	L_s	2.83×10^6	J kg^{-1}
Latent heat of sublimation	L_s	2.83×10^6	J kg^{-1}
Gas constant for dry air	R_d	287.06	J kg^{-1} K^{-1}
Gas constant for vapour	R_v	461.5	J kg^{-1} K^{-1}
Density of liquid water	ρ_l	1000	kg m^{-3}
Molar mass of water	m_v	18.02	g mol^{-1}
Universal Gas Constant	R	8.314	J K^{-1} mol^{-1}
Saturation vapour pressure at $T_0 = 0^o$C	e_{s0}	611.2	Pa
Vapour diffusion coefficient	D	$\approx 2.2 \times 10^{-5}$	m$^2 s^{-1}$
Surface tension of liquid water	$\sigma_{l,v}$	7.5×10^{-2}	Nm^{-1}

Table 2.2: Table of radiation constants

Planetary albedo of Earth	α_p	0.3	
Planetary albedo of Mercury	α_p	0.07	
Speed of light	c	3×10^8	m s^{-1}
Planck Constant	h	6.625×10^{-34}	J s
Boltzmann constant	k	1.3806×10^{-23}	J K^{-1}
Stefan Boltzmann constant	σ	5.67×10^{-8}	Wm^{-2} K^{-4}
radius of the earth	r_e	6340	km
radius of the sun	r_s	0.7×10^6	km
distance between Earth and the Sun	r_d	149.6×10^6	km
distance between Mercury and the Sun	r_d	58×10^6	km
Solar Constant	S_0	1370	W m^{-2}

Index

Bibliography

Berry, E. X., 1967: Cloud droplet growth by collection. *J. Atmos. Sci.*, **24**, 688–701.

Berry, E. X., and R. L. Reinhardt, 1974: An analysis of cloud drop growth by collection Part II. Single initial distributions. *J. Atmos. Sci.*, **31**, 1825–1831.

Demott, P. J., D. J. Cziczo, A. J. Prenni, D. M. Murphy, S. M. Kreidenweis, and D. S. Thomson, 2003: Measurements of the concentrations and composition of nuclei for cirrus formation. *Proc. Nat. Acad. Sci.*, **100**, 14 655–14 660.

Fleishauer, R. P., V. E. Larson, and T. H. Vonder Haar, 2002: Observed microphysical structure of midlevel, mixed-phase clouds. *J. Atmos. Sci.*, **59**, 1779–1804.

Fletcher, N. H., 1962: *The Physics of Rainclouds*. Cambridge Univ. Press, New York, 386pp.

Gierens, K., 2003: On the transition between heterogeneous and homogeneous freezing. *Atmos. Chem. Phys.*, **3**, 437–446.

Gierens, K., U. Schumann, M. Helten, H. Smit, and A. Marenco, 1999: A distribution law for relative humidity in the upper troposphere and lower stratosphere derived from three years of MOZAIC measurements. *Ann. Geophysicae*, **17**, 1218–1226.

Gunn, K. L. S., and J. S. Marshall, 1958: The distribution with size of aggregate snowflakes. *J. Atmos. Sci.*, **15**, 452–461.

Hoose, C., and O. Möhler, 2012: Heterogeneous ice nucleation on atmospheric aerosols: a review of results from laboratory experiments. *Atmospheric Chemistry and Physics*, **12 (20)**, 9817–9854.

Kashchiev, D., 2000: *Nucleation*. Butterworth-Heinemann.

Klett, J. D., and M. H. Davis, 1973: *J. Atmos. Sci.*, **30**, 107–117.

Koop, T., B. P. Luo, A. Tsias, and T. Peter, 2000: Water activity as the determinant for homogeneous ice nucleation in aqueous solutions. *Nature*, **406**, 611–614.

Macke, A., J. Mueller, and E. Raschke, 1996: Single scattering properties of atmospheric ice crystals. *J. Atmos. Sci.*, **53**, 2813–2825.

Marshall, J. S., and W. M. K. Palmer, 1948: The distribution of raindrops with size. *J. Atmos. Sci.*, **5**, 165–166.

Mason, B. J., 1978: Physics of a raindrop. *Physics Education*, **13**, 414–419.

Pruppacher, H. R., and J. D. Klett, 1997: *The Microphysics of Clouds and Precipitation*. Kluwer Academic Publishers, pp. 954.

Quante, M., 2004: The role of clouds in the climate system. *Journal de Physique IV (Proceedings)*, EDP sciences, Vol. 121, 61–86.

Ren, C., and A. R. Mackenzie, 2005: Cirrus parametrization and the role of ice nuclei. *Q. J. R. Meteorol. Soc.*, **131**, 1585–1605.

Rogers, R. R., and M. K. Yau, 1989: *A short course in cloud physics*. Pergamon Press, 290pp pp.

Spichtinger, P., K. Gierens, and W. Read, 2003: The global distribution of ice-supersaturated regions as seen by the Microwave Limb Sounder. *Q. J. R. Meteorol. Soc.*, **129**, 3391–3410.

Tompkins, A. M., K. Gierens, and G. Rädel, 2007: Ice supersaturation in the ECMWF integrated forcast system. *Q. J. R. Meteorol. Soc.*, **133**, 53–63.

Willis, P. T., 1984: Functional fits to some observed drop size distributions and parameterization of rain. *J. Atmos. Sci.*, **41**, 1648–1661.